マイクロマシン技術を応用した術中使用可能な耳小骨可動性測定装置の開発

マイクロマシン技術を応用した術中使用可能な耳小骨可動性測定装置の開発

(11557124)

平成11年度～平成12年度科学研究補助金(基盤研究(B)(2))研究成果報告書

平成14年3月

研究代表者　和田　仁
(東北大学大学院工学研究科教授)

マイクロマシン技術を応用した術中使用可能な耳小骨可動性測定装置の開発

(11557124)

平成11年度～平成12年度科学研究補助金(基盤研究(B)(2))研究成果報告書

平成14年3月

研究代表者　和田　仁
(東北大学大学院工学研究科教授)

研究組織

研究代表者：　和田　仁　（東北大学大学院工学研究科教授）
研究分担者：　小林俊光　（長崎大学大学院医学研究科教授）
研究分担者：　小池卓二　（東北大学大学院工学研究科講師）

交付決定額　（配分額）

	直接経費	間接経費	合　計
平成11年度	5,000	0	5,000
平成12年度	5,000	0	5,000
総　計	10,000	0	10,000

研究発表

(1) 学会発表

Hiroshi Wada, Takuji Koike, Yu Yuasa, Tetsuaki Kawase, and Hiroaki Fujii,
Measurement of stapes mobility in guinea pigs and rabbits,
Hearing Research, 154, (2000), 158-164.

(2) 口頭発表

小池卓二，和田　仁，湯浅　有，湯浅　涼，川瀬哲明，
耳小骨可動性計測装置の開発
Audiology Japan, 2001年10月4日

Takuji Koike, Hiroshi Wada, Yu Yuasa, Ryo Yuasa, Tetsuaki Kawase,
Toshimitsu Kobayashi,
Development of a diagnostic apparatus for stapes fixation,
Association for Research in Otolaryngology, The 25th Annual Midwinter Meeting,
2002年1月27日

Takuji Koike, Hiroshi Wada, Yu Yuasa, Ryo Yuasa, Tetsuaki Kawase,
Toshimitsu Kobayashi,
Hand-guided diagnostic apparatus for stapes fixation,
XXVI International Congress of Audiology,
20002年3月17日

(3) 出版物

な　し

研究成果による工業所有権の出願・取得状況

米国特許仮出願，　番号60/282,336，出願日　2001年4月6日

Contents

Abstract

The ossicular chain, consisting of the malleus, incus and stapes, plays an important role in auditory mechanics. If some part of the ossicles becomes fixed, hearing loss occurs. In order to improve the level of hearing, the fixated part is replaced with a prosthesis. This surgery is called "tympanoplasty". It is important to evaluate the stapes mobility during the tympanoplasty, because it affects the prognosis of improvement of the hearing level. However, objective measurement of stapes mobility has not yet to be achieved.

In this study, an apparatus which is clinically useful for measuring the stapes mobility based on the method of Wada et al. (2000) was developed by assembling a small-sized force sensor and a high-precision actuator, and its clinical applicability was evaluated by measuring stapes mobility in the guinea pig.

Chapter 1. Introduction

The middle ear plays an important role in auditory mechanics, transmitting sound signals efficiently from the ear canal to the cochlea. If some ligaments and tendons which support ossicles become ossified or the ossicles adhere to the wall of the tympanic cavity, the vibration of the ossicles is obstructed and conductive hearing loss occurs. In order to improve the level of hearing, the fixated part must be replaced with a prosthesis in tympanoplasty. In such cases, it is important to evaluate the stapes mobility, because it affects the prognosis of improvement of the hearing level. However, quantitative evaluation of stapes mobility has been difficult to date.

Recently, many investigations on the middle ear function have been reported. A conventional impedance audiometer measures the impedance of the middle ear with a low frequency tone. Here, impedance is expressed as the ratio of a force-like quantity (pressure) to a velocity-like quantity (volume velocity of the tympanic membrane), and is a measure of the resistance to the flow of energy into the system. This method is valuable for the diagnosis of secretory otitis media, but it is insufficient for the diagnosis of ossicular chain disorders (Jeger et al., 1974; Bel et al., 1975; Browning et al., 1985; Gersdorff and Stoquart, 1985). To diagnose such disorders, a three-dimensional sweep frequency impedance meter (3D SFI) with a probe-tone sweep frequency of 0.1 kHz to 2.0 kHz was developed, which proved to be a powerful tool for diagnosing ossicular chain disorders (Wada et al., 1998). However, as the equipment measures the impedance at the tympanic membrane, it is difficult to judge the locations of such disorders (Jeger et al., 1974; Browning et al., 1985; Wada et al., 1998). Therefore, direct observation of stapes movement is indispensable for evalu-

ation of stapes mobility.

The mobility of each part of the ossicles has been investigated directly by the Mössbauer technique using a gamma-ray (Lynch et al., 1982; Gummer et al., 1989; Ruggero et al., 1990), a video measuring system (Gyo et al., 1987), a optical measuring system (Merchant et al., 1996), a laser Doppler vibrometer (Stasche et al., 1994; Kurokawa et al., 1995; Schon et al., 1999; Heiland et al., 1999) and a heterodyne interferometer (Decraemer et al., 2000). Although movement of the ossicles can be measured at the nanometer level with these methods, the required equipment is large, posing difficulties for use in surgery.

Wada et al. (2000) have developed a simple sensor for measuring the load and displacement of stapes. In this study, the slope of the load-displacement curve was used as an index of the stapes mobility, and a significant difference was found between the stapes mobility of the normal and fixed stapes. However, the size of the sensor was still large and its shape was unsuited for use during the surgery. In this study, a new apparatus for measurement of stapes mobility based on the method of Wada et al. (2000) was developed by assembling a small-sized force sensor and a high-precision actuator, and its clinical applicability was evaluated by measuring the stapes mobility of guinea pigs.

Chapter 2. Function and pathology of middle ear

Figure 2.1 shows a schematic of the human ear. The ear consists of three parts, the outer ear, the middle ear, and the inner ear. The inner ear consists of two parts, the vestibular apparatus for balance and the cochlea for hearing. The outer ear and middle ear conduct sound to the cochlea, which separates sounds with regard to frequency before they are transduced into a neural code in fibers of the auditory nerve.

The middle ear consists of the tympanic membrane, which terminates the ear canal, and three small bones (ossicles), i.e., the malleus, incus and stapes. These ossicles are wrapped in a bone structure called the tympanic cavity, which is filled with the air. The manubrium of the malleus is imbedded in the tympanic membrane and the head of the malleus is connected to the incus, which in turn connects to the stapes, the footplate of which is located in the oval window of the cochlea. The ossicles are supported by several ligaments. Particularly, the stapes is supported by the annular ligament which exists in the gap between the footplate of the stapes and the oval window.

Figure 2.2 shows a schematic of a guinea pig ear. The auditory system of guinea pigs is also divided into three parts as in humans. The middle and inner ear of the guinea pig are wrapped in a bone structure called the bulla. The ossicular chain of guinea pigs also consist of the malleus, the incus, and the stapes. However, the malleoincudal joint is not as clear as that in humans.

Because of the difference in the impedance of the two media, air and lymph fluid in the inner ear, if there were no middle ear, about 99.9% of the sound energy

would be reflected at the interface between air and lymph fluid and only 0.1 % of the energy would be converted into vibrations of the lymph fluid. The malleus and the incus are shaped like a lever. In case of humans, the ratio of the lever is about 1.3, and the ratio of the area of the tympanic membrane to the area of the stapes footplate is about 15.6 (Kirikae, 1960). Therefore, the sound pressure in the air is amplified by 20 times and then delivered to the lymph in the inner ear by the middle ear. In this way, the middle ear acts as an impedance transformer that matches the high impedance of the cochlear lymph fluid to the low impedance of air.

Otosclerosis is a disorder of bone growth that affects the stapes and the bony labyrinth of the cochlea. The disease process is characterized by resorption of the normally hard bone, which is replaced by a newer, softer bone tissue that is highly vascularized and spongy. This spongy bone can eventually turn into a dense sclerotic mass. These pathologic changes prevent the stapes from vibrating in response to sounds, thus leading to progressive conductive hearing loss up to 50 dB (Schuknecht, 1971; Goodhill, 1979). An example of an audiogram obtained from a patient with otosclerosis is shown in Figure 2.3 (Kirikae and Nomura, 1987). Although the bone conduction is normal, the hearing loss of air conduction characteristically first affects the low frequencies. Moreover, loss in the high frequencies appears with progression of the disease (Schuknecht, 1971; Goodhill, 1979; Hannley, 1993). Shuknecht (1971) suggested that the degree of conductive hearing loss appeared to be determined by the stage of stapes footplate fixation. The first stage, fibrous fixation of footplate, is thought to be the initial pathological change resulting in conductive hearing loss of $\leqq$ 30 dB. The second stage, localized bony fixation of anterior part of the footplate, is thought to result in conductive hearing loss of 30 to 40 dB. The final stage, diffuse

bony ankylosis involving the entire circumference of annular ligament, is suggested to result in a conductive hearing loss over 40 dB. However, the quantitative relationship between the conductive hearing loss and degree of stapes footplate fixation has not been well clarified.

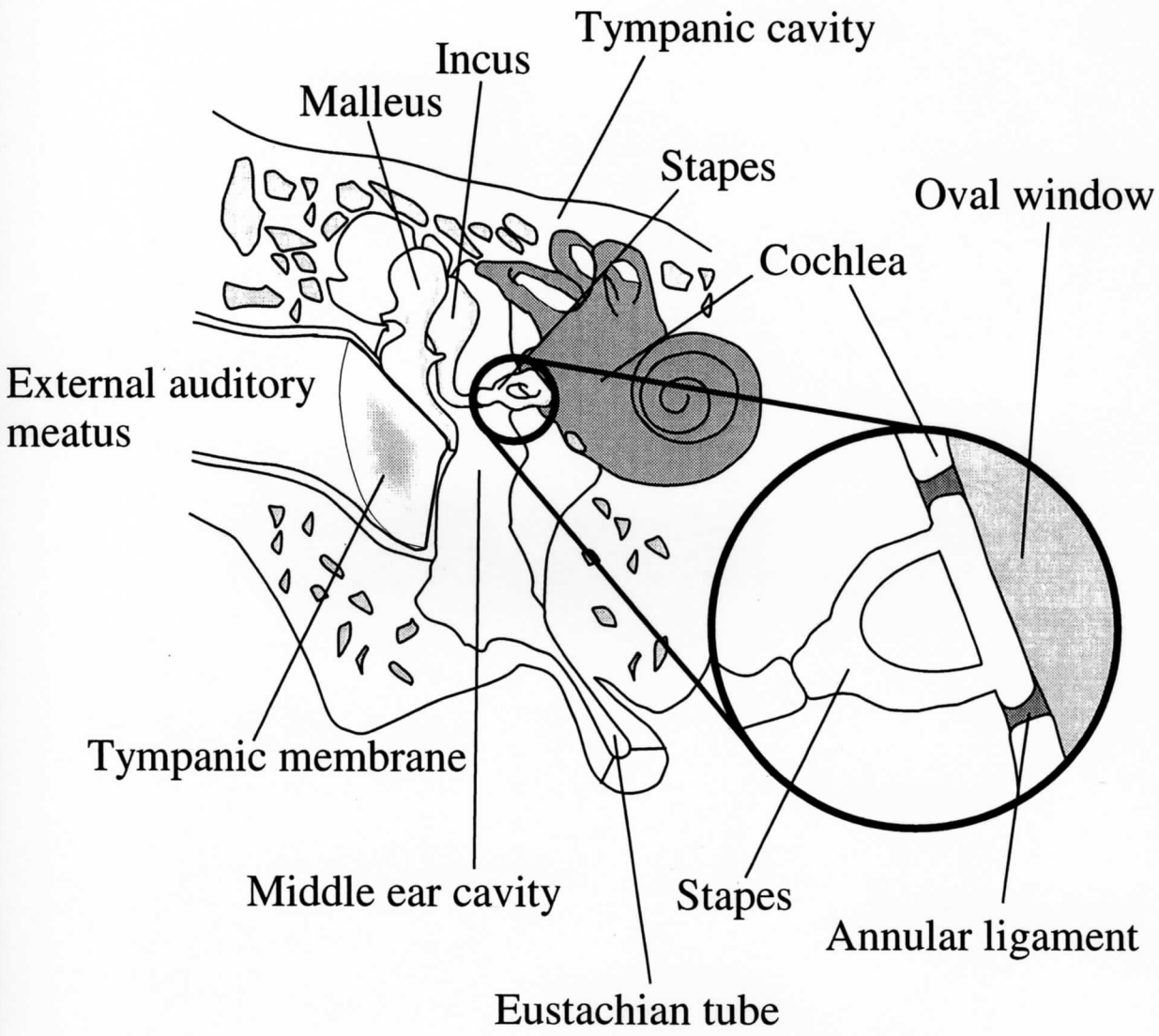

Fig. 2.1. Schematic of the human auditory system.

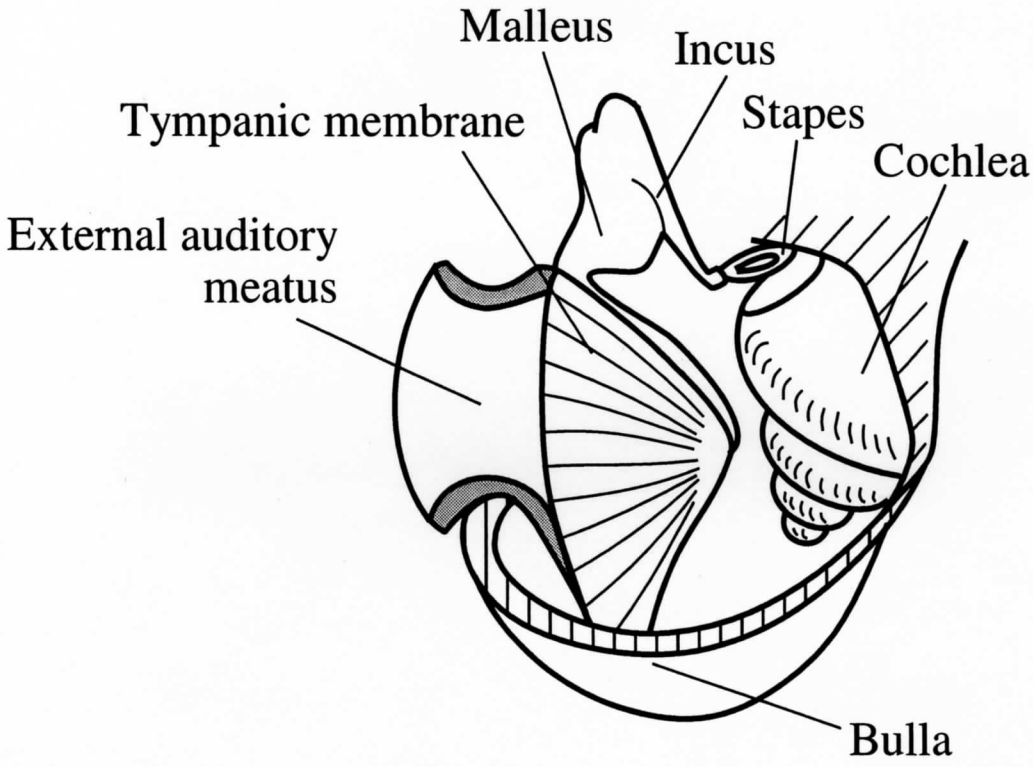

Fig. 2.2. Schematic of the guinea pig auditory system.

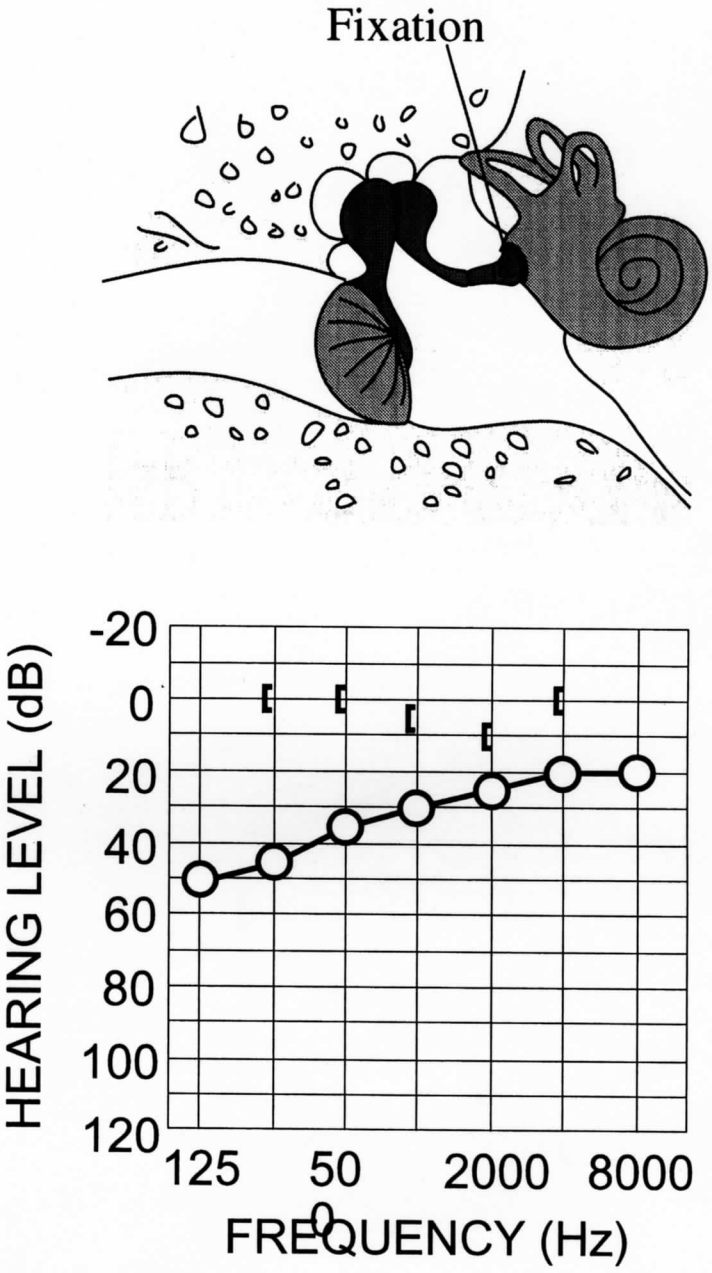

Fig. 2.3. An audiogram obtained from a patient with otosclerosis (Kirikae and Nomura, 1987). ○, air conduction; [, bone conduction. Although bone conduction is normal, hearing loss of air conduction characteristically first affects the low frequencies. Moreover, the hearing loss increases in severity and progressively involves the high frequencies (Schuknecht, 1971; Goodhill, 1979; Hannley, 1993).

Chapter 3. Design of the apparatus

3.1. Pilot experiments

As a pilot experiment, measurement of stapes mobility using a simple sensor for measuring the load and displacement of stapes was done by Fujii (2000) and Wada et al. (2000).

3.1.1. Measurement system used in the pilot experiments

Figure 3.1 shows photographs of a simple load-displacement sensor and measurement system. The sensor is composed of two parts (Fig. 3.2). One is an actuator, consisting of two piezoelectric bimorphs (Murata PKF02C5) to generate displacement of the stapes, and the other is an aluminum beam to measure the load of the stapes. Strain gauges (KYOWA KFG-02-120-C1-11 L1M2R), which can convert strain to change of electric resistance, are bonded to both sides of the actuator and the beam. The needle that comes in contact with the stapes is placed on one end of the beam, and the other end of the beam is fixed to a plastic block. The actuators are connected to the plastic block by brass plates, which are flexible and easily bent.

Figure 3.3 is a block diagram of the measurement system. Once the needle touches the stapes, the actuator, which is controlled by a computer through the General Purpose Interface Bus (GPIB), begins to bend down and the beam is simultaneously bent up by the reaction force from the stapes. Each voltage change that is generated in the bridge box is amplified by a dynamic strain amplifier (KYOWA DPM-603A) and converted into a digital signal (Interface IBX-3113). All data are stored in a personal computer.

As shown by Fig. 3.4, both displacements of the actuator (D_1) and the beam (D_2) are detected by the voltage changes that are generated in the bridge box, if the relationships between D_1 or D_2 and detected voltage have been previously calibrated (Wada et al., 2000). The displacement of the stapes (X) can be calculated by $D_1 - D_2$. The beam can simultaneously detect the load applied to the stapes, which is equal to the reaction force (F), if the relationship between D_2 and F has been also calibrated (Wada et al., 2000). Stapes mobility is evaluated by the relationship between the load applied to the stapes and the displacement of the stapes.

3.1.2. Measurement of the stapes mobility using a simple sensor

Guinea pigs (Fig. 3.5) weighing between 0.25 and 0.50 kg (postnatal age 4 – 8 weeks) were examined. Measurement was done *in vivo* (Wada et al., 2000).

The sensor that was mounted on the manipulator was set so that the needle of the sensor was vertical against the footplate of the stapes. If the needle come in contact with the stapes head, the computer began to collect data of the displacement and load of the stapes. The displacement was given till 5.0 to 6.0 $\times$ 10^{-3} N. It took about 30 sec to measure the stapes mobility in one animal. After the measurement of the normal stapes mobility, the stapes was artificially fixed with a small amount of alkyl–α–cyanoacrilate glue which was applied to the footplate and the annular ligament. The fixed stapes mobility was also measured with this sensor.

3.1.3. CM measurement

The cochlear microphonics (CM) amplitude before and after fixation of the

stapes was measured to estimate the relationship between the change of mobility and the change of sound pressure transmitted to the cochlea, as shown in Fig. 3.6. Because the relationship between the CM amplitude and the sound pressure transmitted to the cochlea is linear (Avan et al., 1992), the degree of artificial fixation, i.e., hearing loss caused by the fixation, is estimated by the change of the CM amplitude before and after the fixation. A piezoelectric vibrator (Rion), which has been employed in an implantable hearing aid, was used to vibrate the stapes. A positive electrode made of silver wire was applied to the round window membrane and a negative electrode and ground electrode were applied to the anterior part of the bulla and the center of the neck, respectively. The vibration consists of 20 ms tone bursts with rise and decay times of 0.5 ms at sound frequencies of 0.5, 1.0, and 4.0 kHz.

3.1.4. Relationship between the load and displacement of the stapes in guinea pigs

Figure 3.7 shows an example of the relationship between the load and displacement of the normal stapes in a guinea pig. The displacement increased linearly with an increase in load in the small displacement region, but nonlinearly increased in the large displacement region. When a sound pressure of 60 – 80 dB SPL was presented to the tympanic membrane, the displacement amplitude of the stapes was scores of nanometers (Kiriake, 1960). However, in this measurement, such a small displacement of the stapes was difficult to evaluate. Therefore, the regression line of the relationship between the load and displacement in the region under 1.0×10^{-3} N was computed by the minimum square method, and its slope, i.e., the equivalent stiffness, was used for evaluating stapes mobility. The equivalent stiffness in Fig. 3.7 was 18

N/m.

The measurements were performed on 30 guinea pigs. All the measurement results are within the hatched areas shown in Fig. 3.8. The averaged values of the equivalent stiffness obtained from 30 guinea pigs was 16 ± 7 N/m. In these measurements, the correlation coefficients of the regression lines ranged from 0.97 to 0.99.

Figure 3.9 shows the change of the equivalent stiffness before and after the artificial fixation of the stapes in a guinea pig. The change of the CM amplitude before and after fixation in this animal is shown in Fig. 3.10. The CM amplitude changed from 460 μV to 32 μV. After the fixation the equivalent stiffness changed from 18 N/m to 55 N/m, in other words, a significant difference was detected between their results.

Figure 3.11 shows the relationship between the change of the CM amplitude and the equivalent stiffness at frequencies of 0.5, 1.0 and 4.0 kHz in eight guinea pigs. The gray area is the average ± standard deviation in the normal stapes. The black circles represent the data of the normal stapes and the white circles are those of the fixed stapes. When the stapes was artificially fixed with glue, the equivalent stiffness increased and the CM amplitude decreased. All data of the fixed stapes were larger than the value of the average + standard deviation in the normal stapes. This result shows that the fixed stapes, which decreases the sound pressure transmitted to the cochlea, can be detected by measuring the equivalent stiffness of the stapes.

3.1.5. Effect of hand trembling

For clinical application, the sensor should be held in the hand (Fig. 3.12).

However, when the stapes mobility is measured with a hand held sensor, hand trembling may be interpreted as loud noise in stiffness measurement. Conducting measurement of stiffness winthin a short time is considered to be a solusion to avoiding the influence of the hand trembling. Figure 3.13 shows relationship between the load and displacement of the normal stapes in a guinea pig with the sensor supported by the micromanipulator and held in the hand. The measurement time required for reducing the effect of the hand trembling was 20 msec.

3.2. Mechanism

3.2.1. Specifications for the new apparatus

From the data obtained in the pilot experiments and other studies, specifications required for a force sensor to measure the stapes mobility of human were determined. Table 3.1 shows specifications. The necessary range of measurement of the reaction force from the stapes of guinea pigs was to 5×10^{-3} N in the pilot experiments. The stapes stiffness in human or human cadavers was 10 to 100 times greater than that of guinea pigs (Mach and Kessel., 1874; Békésy, 1960; Kirikae, 1960; Onchi, 1961; Zwislocki, 1962). Furthermore, Hüttenbrink (1993) measured the stapes stiffness of human cadavers at the rupture of the annular ligaments, which was 580 N/m and 30 times stiffer than the stapes stiffness of guinea pigs. Therefore, it was expected that the necessary range of measurement of the reaction force from the stapes of human was at least 10 times as large as that of guinea pigs. However, if the range of measurement of the reaction force is set too large, the sensitivity of a force sensor becomes low. Consequently, the rated force of a force sensor was determined to be 50×10^{-3}

N. The accuracy, $\pm$ 0.2 $\times$ 10^{-3} N was required to have the same sensitivity as the simple sensor. The size of a force sensor must be small to keep a wide visual field because it is inserted into the external auditory meatus.

Table 3.2 shows the specifications, based on polot experiments, of an actuator to measure the stapes mobility in humans. Maximum displacement and displacement accuracy were determined to be the same as those of the actuator used in the pilot experiments. The allowable frequency was set at 10 Hz to reduce the effect of hand trembling.

According to these specifications, the capacitive force sensor, which has high accuracy and can easily be miniaturized, was chosen for use as the sensor. The capacitive force sensor was newly designed, and the hydraulic micromanipulator (NARISHIGE MO-81) was improved for use as the actuator.

3.2.2. Schematic of the apparatus

Figure 3.14 shows a schematic of the apparatus for measuring the stapes mobility in human which was newly designed in this study. The apparatus consists of a probe and a grip (Fig. 3.14 (a)). It is used by inserting the probe part into the external auditory meatus. Surgery must be done in a narrow visual field, 10 to 15 mm in diameter when the external auditory meatus is cut open, and the circumference of the probe, therefore, should be small. In this study, the diameter of the probe was designed to be 3 mm. Because the direction perpendicular to the footplate is at a 20 degrees angle with the direction of the external auditory meatus, the push rod and its direction of movement have to be tilted by 20 degrees to push the stapes vertically.

A force sensor with a push rod was installed in the tip of the probe part, and

connected to a hydraulic micromanipulator (NARISHIGE, MO-81 customized) which was used as an actuator through a flexible coil spring and wires (Fig. 3.14 (b)). Fig. 3.15 shows the photographs of the apparatus.

3.2.3. Principle of measurement

Figure 3.16 shows the principle of measurement. Once the push rod touches the stapes, the moving part with the sensor and push rod, which is connected to a hydraulic micromanipulator through a flexible coil spring and wires, is moved backward and forward under the control of the computer. While the sensor is moved, the reaction force (F) which the sensor receives from the stapes is measured and the data is stored in the computer. When a load is applied to the sensor, deflection of the sensor diaphragm occurs. However, as the stiffness of the sensor diaphragm, about 1.5×10^4 N/m, is sufficiently stiffer than that of the stapes measured by direct pushing in human cadavers (Hüttenbrink, 1993), 580 N/m, the deflection is negligible. Therefore, stapes displacement is considered to be equal to the displacement of the moving part (X). The stapes mobility is determined by the relationship between the values of F and X.

3.3. Sensor

3.3.1. Design of the sensor

In this study, the force sensor for measuring stapes mobility was designed based on the occlusal force sensor (Nozaki et al., 2000). According to specifications for a force sensor (Table 3.1), the top view of the sensor is set to be 2 by 2 mm square

(Fig. 3.17). The sensor has a structure consisting of a p^+ silicon rigid-center round diaphragm and a pyrex glass with an electrode pattern. This force sensor has two capacitors, C_1 and C_2, which have the same capacitances when the diaphragm is unloaded. The C_2 is changed by load, although the C_1 is unchanged. A small difference between these capacitances is detected using a diode bridge circuit.

The property of the sensor is almost completely dependent on the diaphragm thickness, h, and the gap between the diaphragm and the electrode, d. Especially, the deflection of a rigid-center diaphragm is inversely proportional to h cubic (Giovanni, 1982; Matsumoto and Esashi, 1993). The parameters h and d were provisionally determined based on Nozaki's sensor and the above reports. Further, as shown in Fig. 3.18, computer simulations using the finite-element method (FEM) were done to determine these dimensions and the electrode pattern on the glass. The parameters h and d were set so that the deflection of a rigid-center and d became equal when 50×10^{-3} N was applied to the diaphragm of the sensor. Consequently, the parameters h and d was set to be 10 μm and 4 μm, respectively.

3.3.2. Making of the sensor

Figure 3.19 shows the fabrication process of the sensor using the micromachining technique (Esashi et al., 1992). The sensor is made from 300 μm thick p^+ silicon and 300 μm thick pyrex glass. (1) Silicon dioxide was deposited on both sides of the p^+ silicon by wet oxidation. (2) After a patterning of silicon dioxide, the back side of the p^+ silicon was etched 4 μm in depth in Tetra Methyl Ammonium Hydroxide (TMAH) to make the gap of sensor. (3) After a patterning of silicon dioxide and a photoresist mask, the front side of the p^+ silicon was etched in Reactive Ion Etching (RIE) to

make the rigid-center part. (4) After exfoliating the photoresist mask, the front side of the p^+ silicon was etched in RIE again to make diaphragm, and the diaphragm thickness was adjusted in this process. (5) Al was sputtered on the front side of the pyrex glass. (6) Then, Al was patterned to make the metal electrode. (7) Finally, the p^+ silicon and the pyrex glass were anodically bonded, and then dicing and wiring were done.

Figure 3.20 shows photographs of the force sensor before wiring. The electrode patterns in the back view from inside to outside are a variable capacitor pattern, a pattern which restrains bonding of the diaphragm, a fixed capacitor pattern and a ground pattern, respectively.

3.3.3. Measurement system using the new apparatus

Figure 3.21 shows the capacitance detector and the circuit of amplifier. The sensor is represented as the capacitors in the gray area. The difference between the capacitances C_1 and C_2 is transformed to output voltage in the detector circuit for capacitance (Harrison and Dimeff., 1973). Then, the output voltage is amplified by the three amplifier circuits. The maximum amplification is $11 \times 12 \times 11$ times. The amplification is adjusted so that the output voltage is 400 to 600 mV when load of 10×10^{-3} N is paalied to the sensor.

Figure 3.22 shows a photograph of the measurement system using the apparatus. The hydraulic micromanipulator installed in the apparatus is controlled by computer through the control unit (Fig. 3.23). The output voltage is stored in the computer through an A/D board.

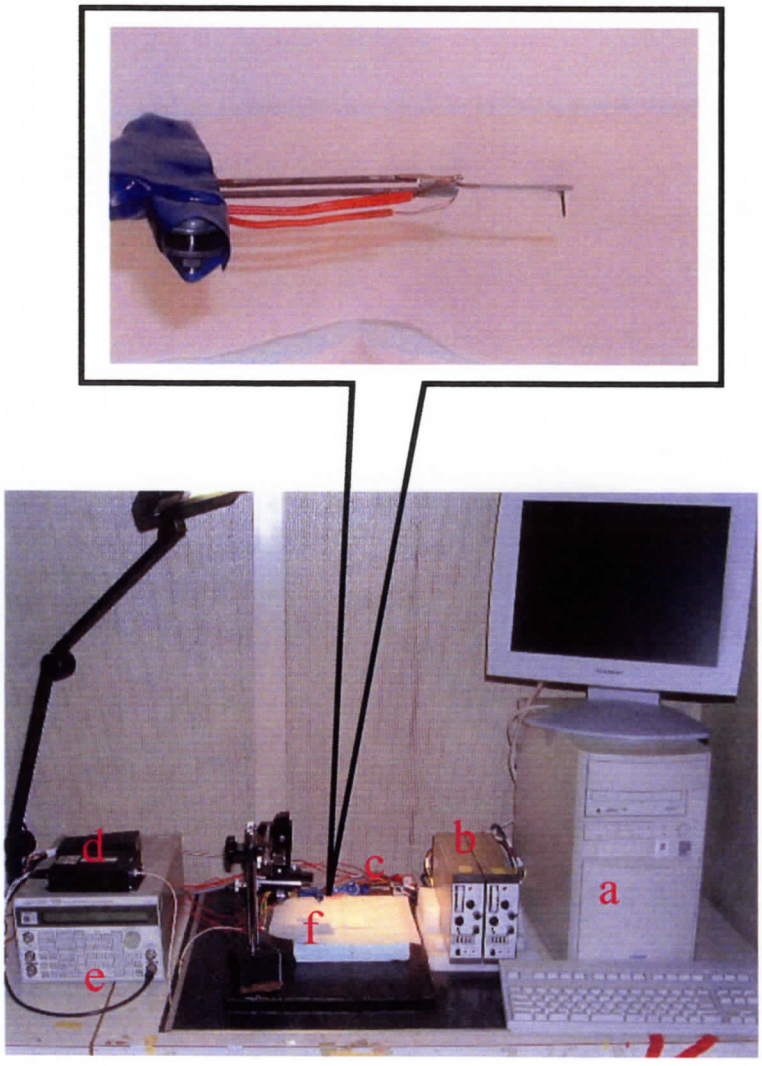

Fig. 3.1. Photographs of a simple load-displacement sensor and measurement system. a, computer; b, dynamic strain amplifiers; c, bridge boxes; d, amplifier; e, multi-function synthesizer; f, sensor.

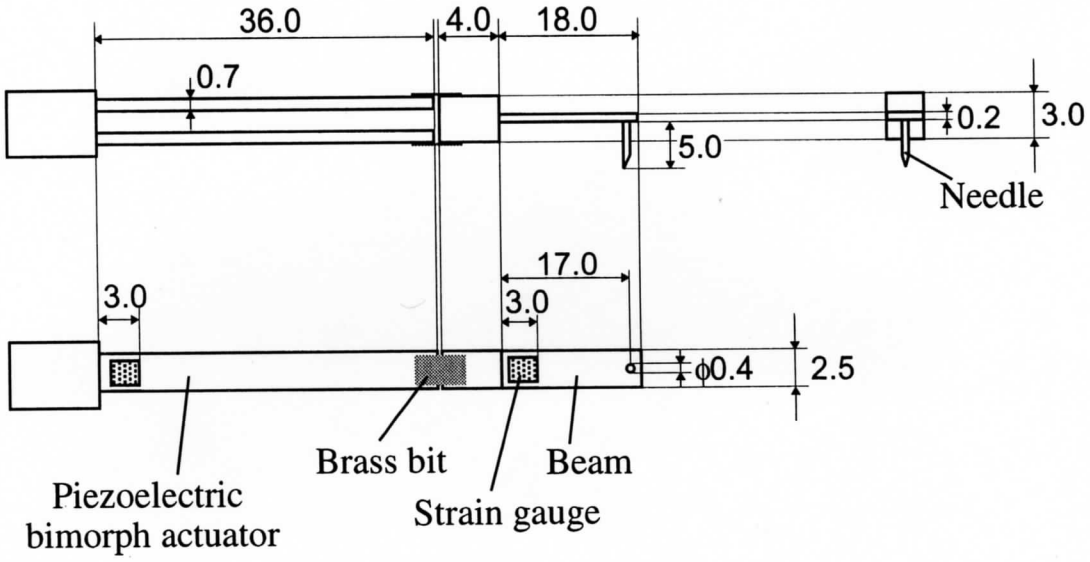

Fig. 3.2. Schematic illustration of the simple load-displacement sensor. Units in millimeters (mm). The scale is different according to the respective parts.

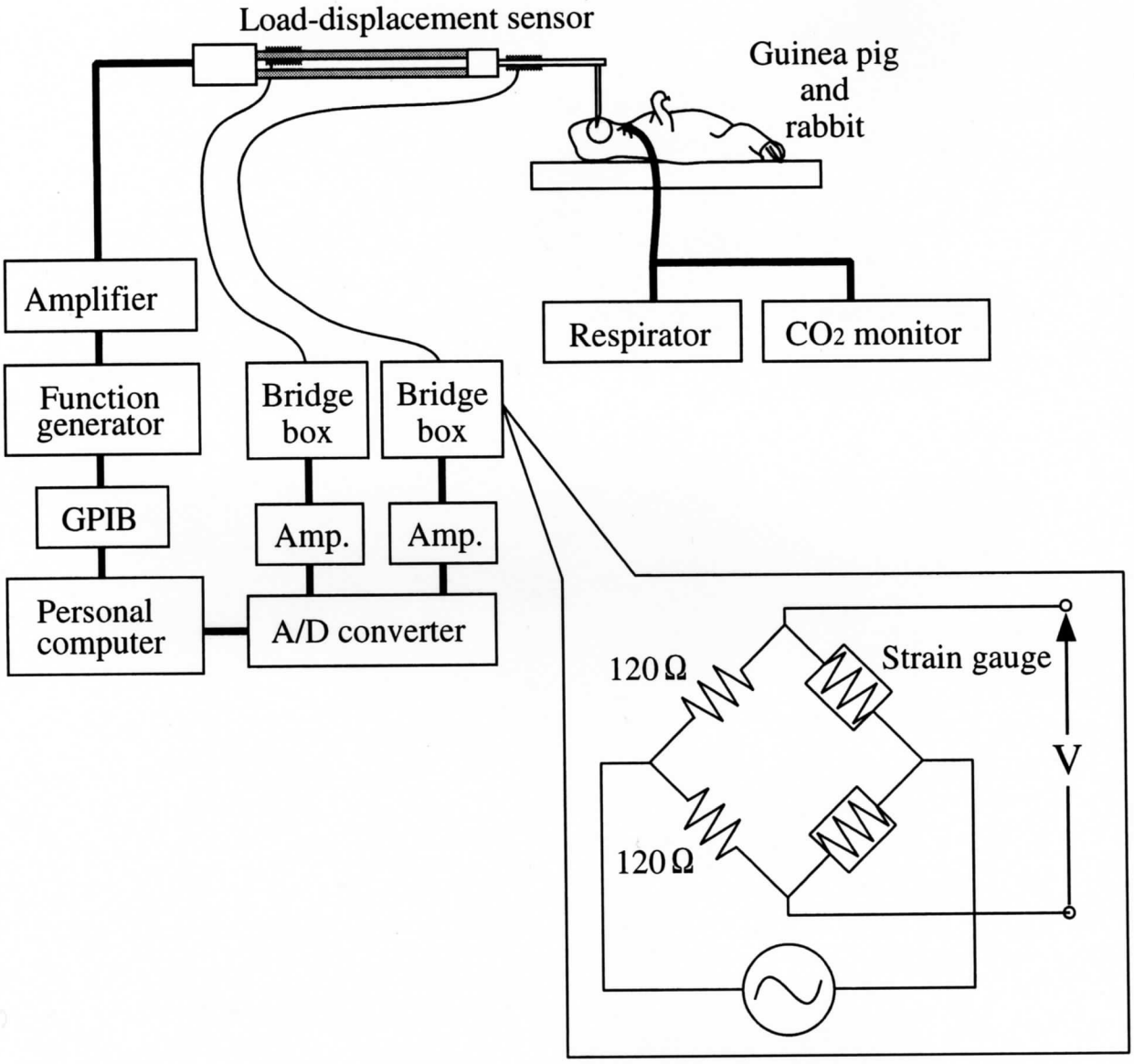

Fig. 3.3. Block diagram of the system for measurement of stapes mobility using a simple load-displacement sensor.

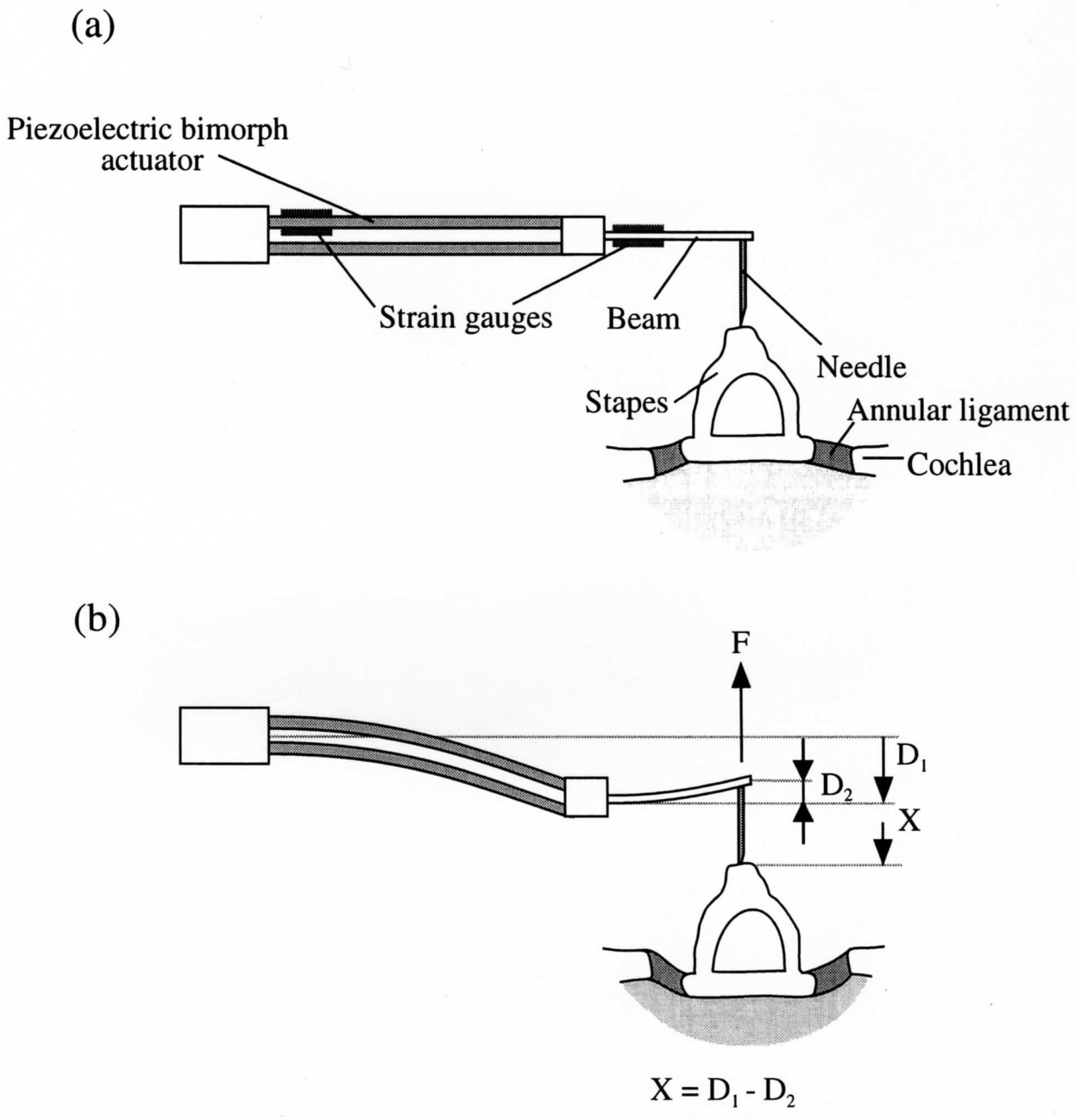

Fig. 3.4. Principle of measurement using a simple load-displacement sensor. (a) Before pushing the stapes. (b) While pushing the stapes. F is the reaction force from the stapes. D_1 and D_2 are the displacement of the actuator and beam, respectively, and $D_1 - D_2$ is equal to the stapes displacement, X.

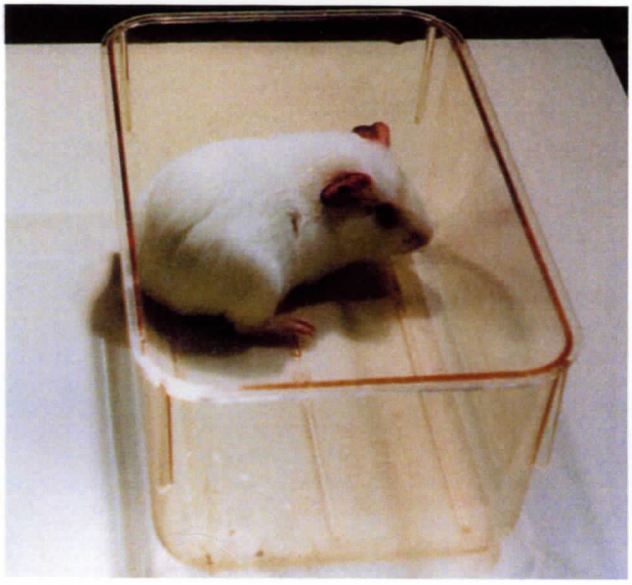

Fig. 3.5. An unpigmented guinea pig.

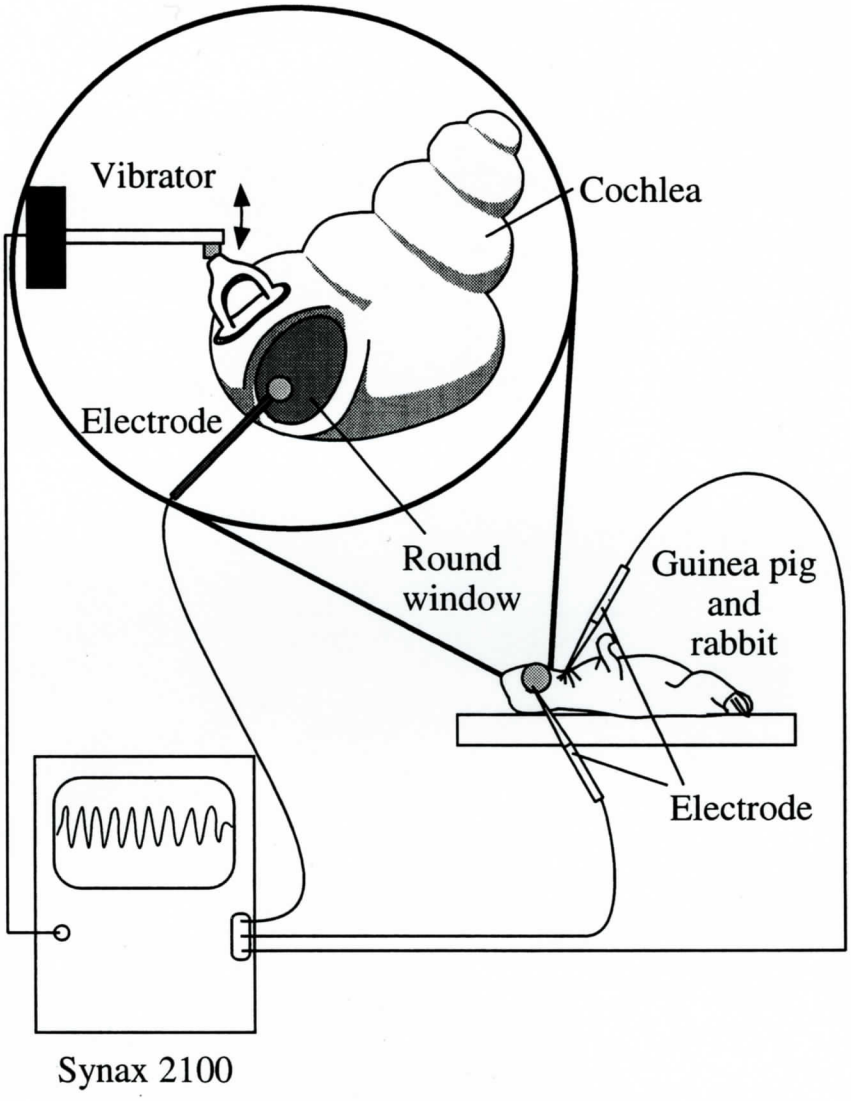

Fig. 3.6. Diagram of CM measurement. The stapes was vibrated by the vibrator. The CM was recorded from the three electrodes: on the round window (+), at the anterior side of the bulla (-), and at the muscle near the neck (GND).

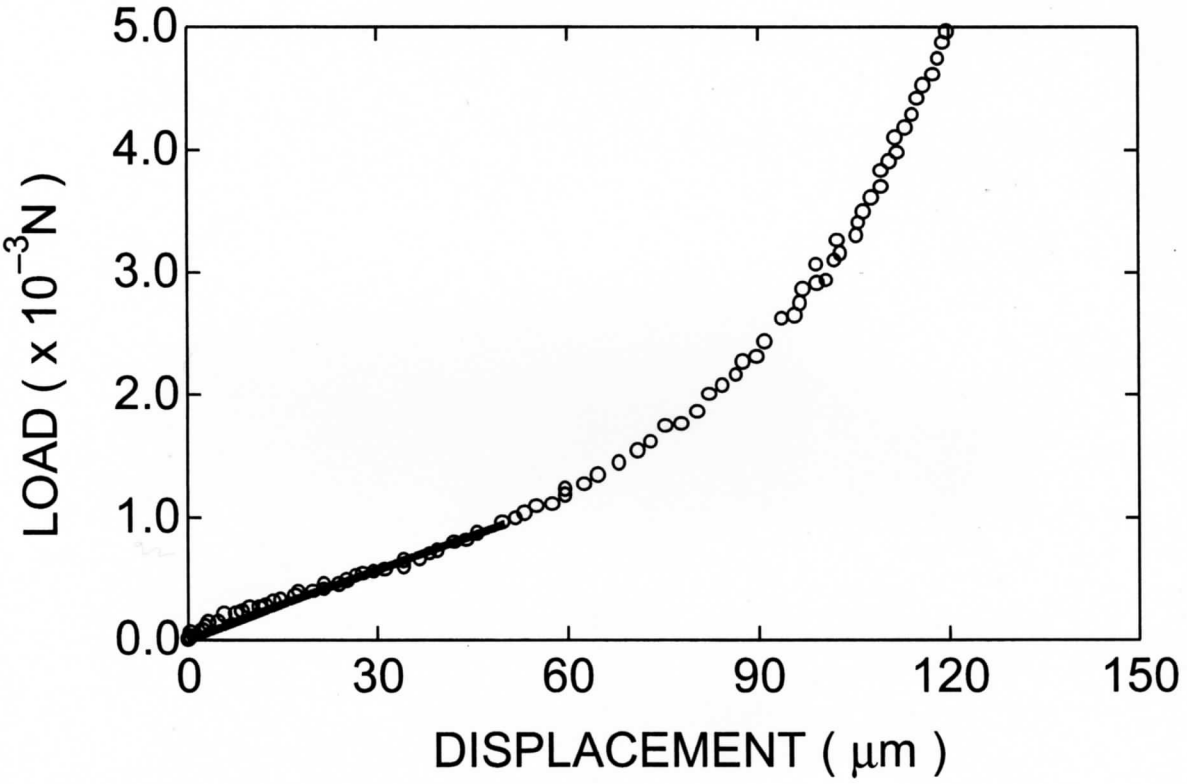

Fig. 3.7. Relationship between the load and displacement of the normal stapes in a guinea pig measured as a pilot experiment. The simple sensor was supported by the micromanipulator. It took about 30 sec in the measurement. The equivalent stiffness 18 N/m was obtained from the regression line, and the correlation coefficient was r = 0.99.

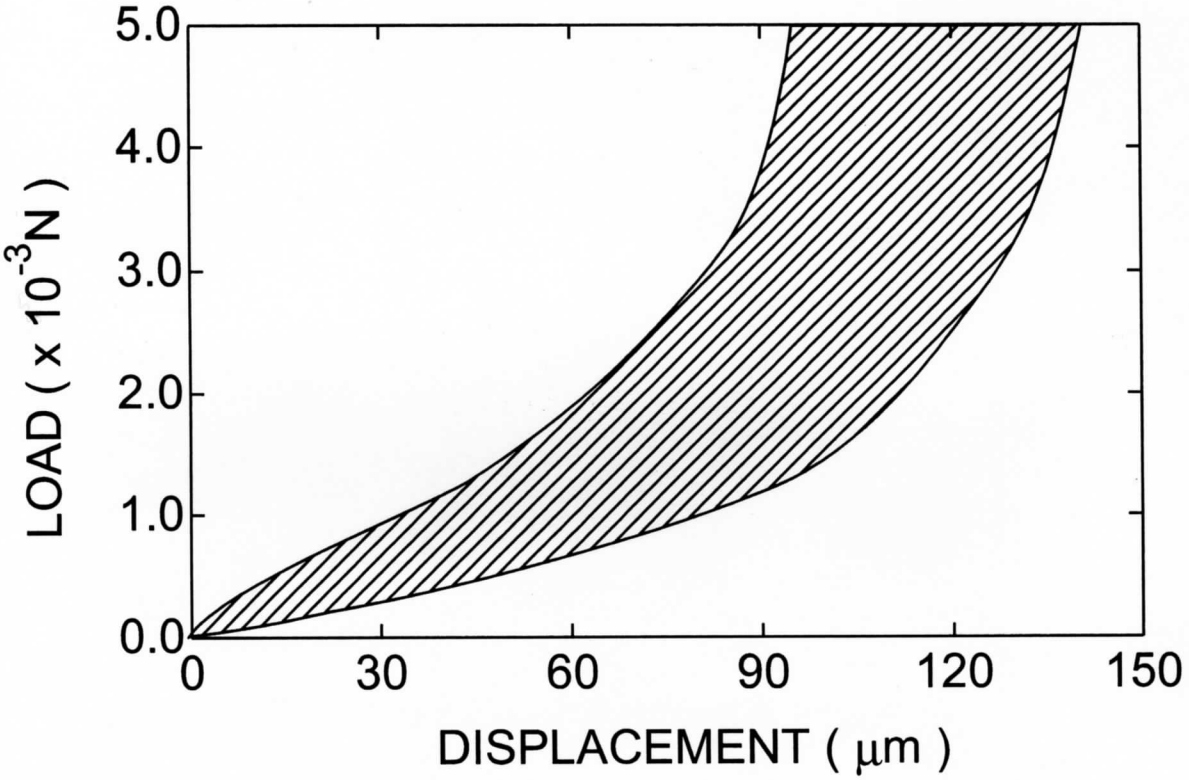

Fig. 3.8. Relationship between the load and displacement of normal stapes in 30 guinea pigs measured as pilot experiments. The simple sensor was supported by the micromanipulator. It took about 30 sec in the measurements. All the measurement results were found within the hatched areas. The average equivalent stiffness of all results was 16 ± 7 N/m.

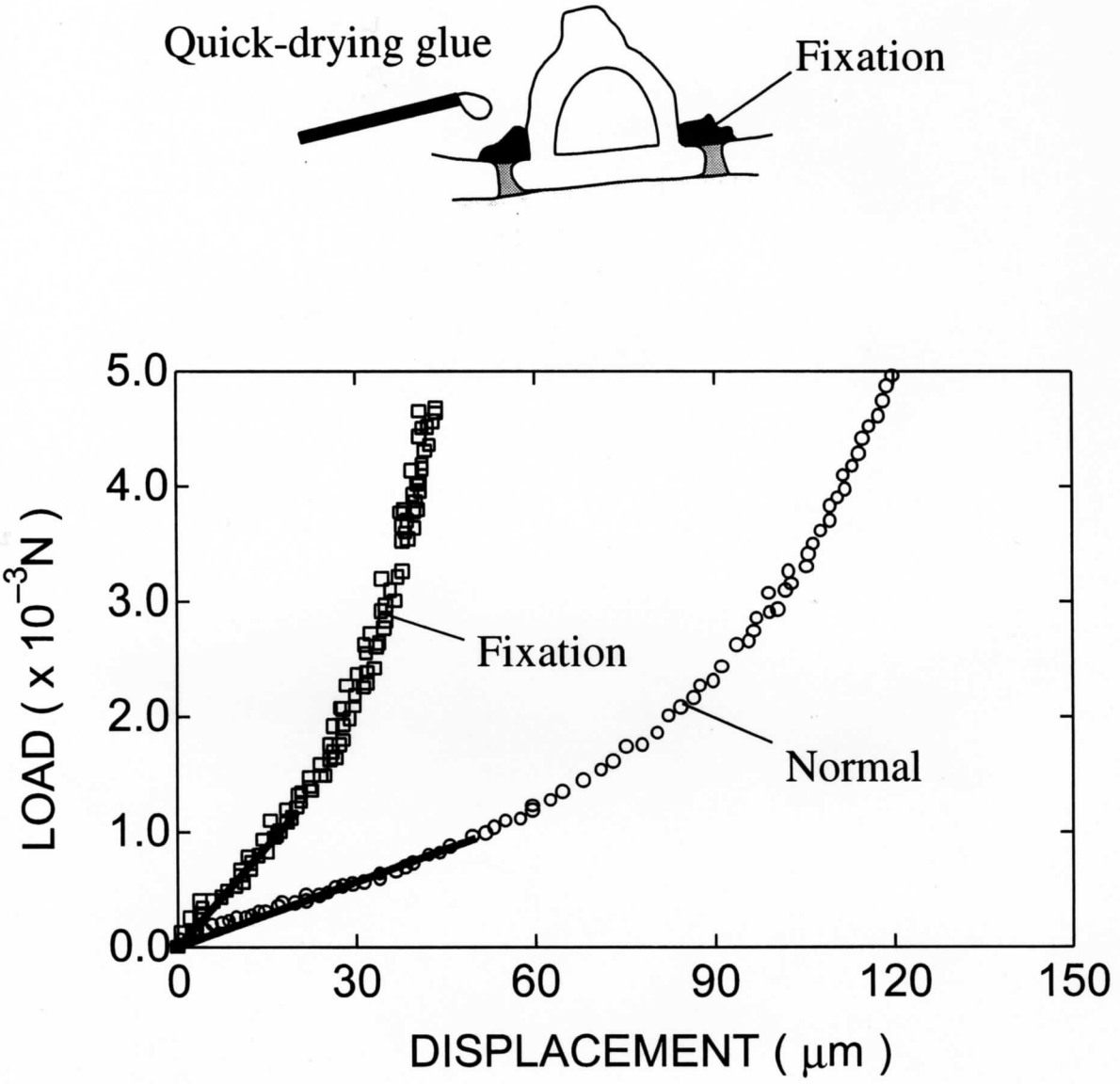

Fig. 3.9. Relationship between the load and displacement of the normal and artificially fixed stapes in a guinea pig measured as pilot experiments. The upper illustration shows the method of realizing the stapes fixation. The simple sensor was supported by a micromanipulator. Measurements took about 30 sec. The equivalent stiffness was 18 N/m in the normal and 55 N/m in the fixation.

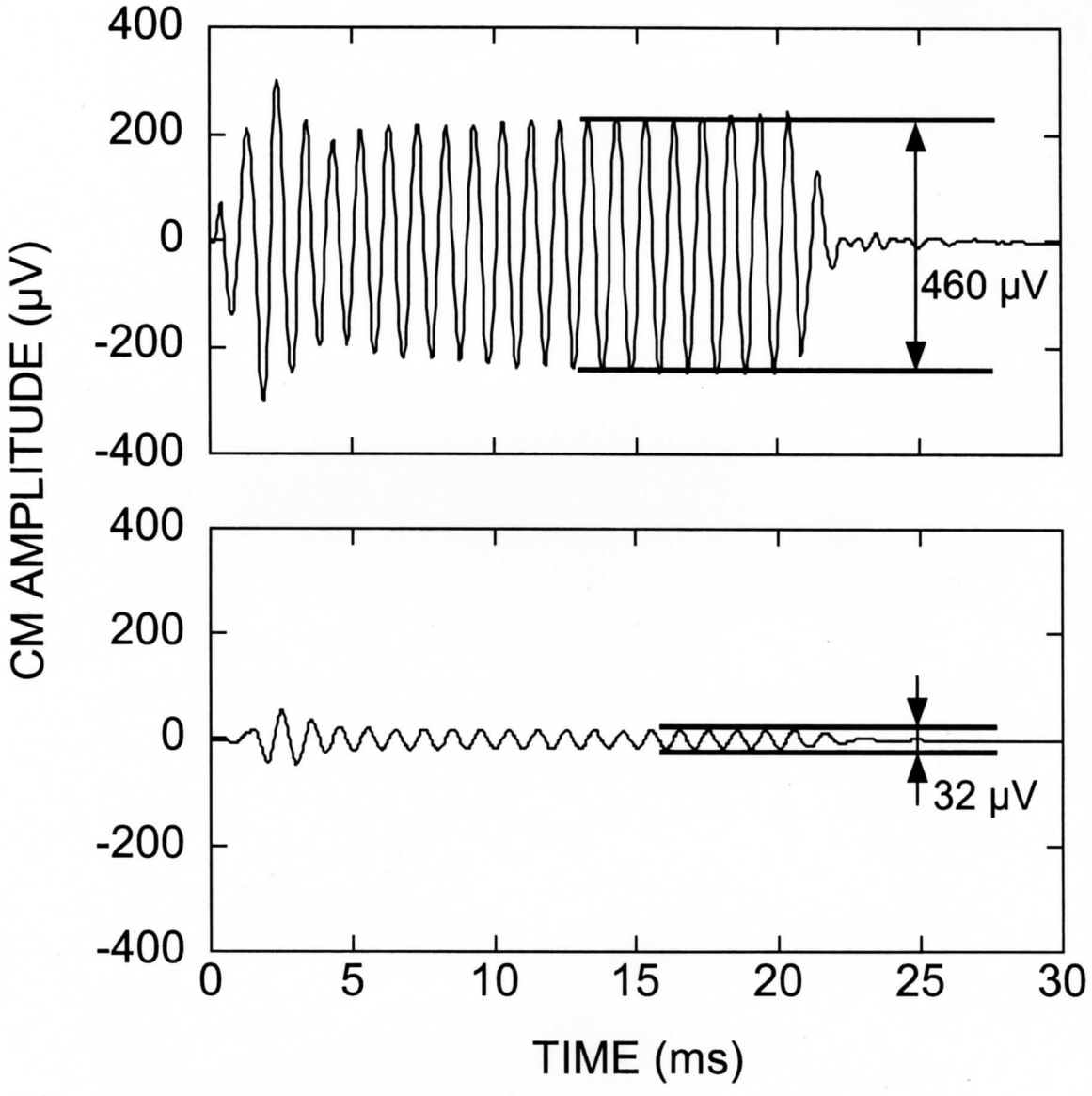

Fig. 3.10. Change of the CM amplitude before and after artificial fixation of the stapes. After fixation, the CM amplitude decreased from 460 μV (a) to 32 μV (b). The vibration applied to the stapes was a 1.0 kHz tone burst.

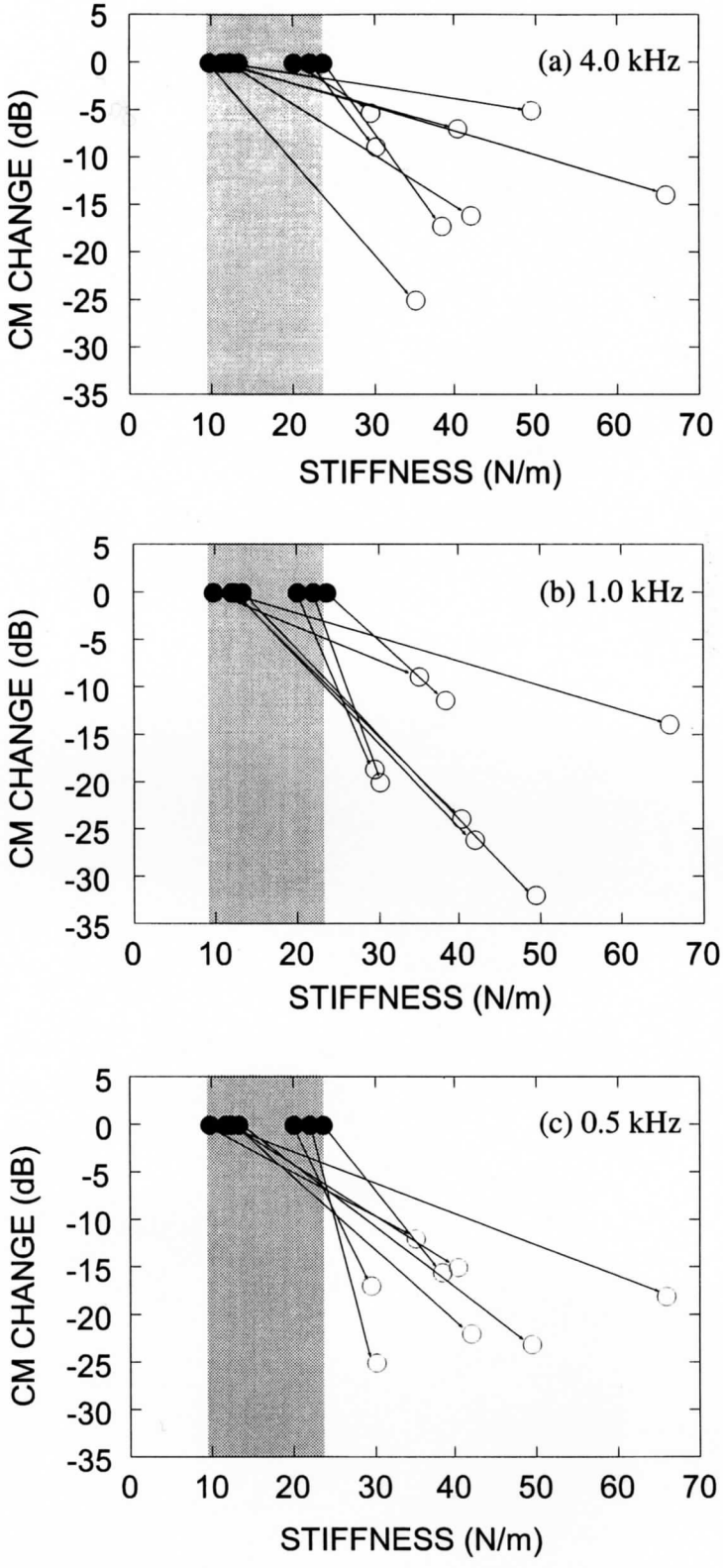

Fig. 3.11. Relationship between the equivalent stiffness and the CM change in guinea pigs while the CM frequency was (a) 4.0 kHz, (b) 1.0 kHz, (c) 0.5 kHz. The gray area is the average ± standard deviation in the normal stapes. The black circles represent the data of the normal stapes and the white circles are those of the fixed stapes. All of the equivalent stiffnesses of the fixed stapes were larger than the range of the average +standard deviation in the normal stapes.

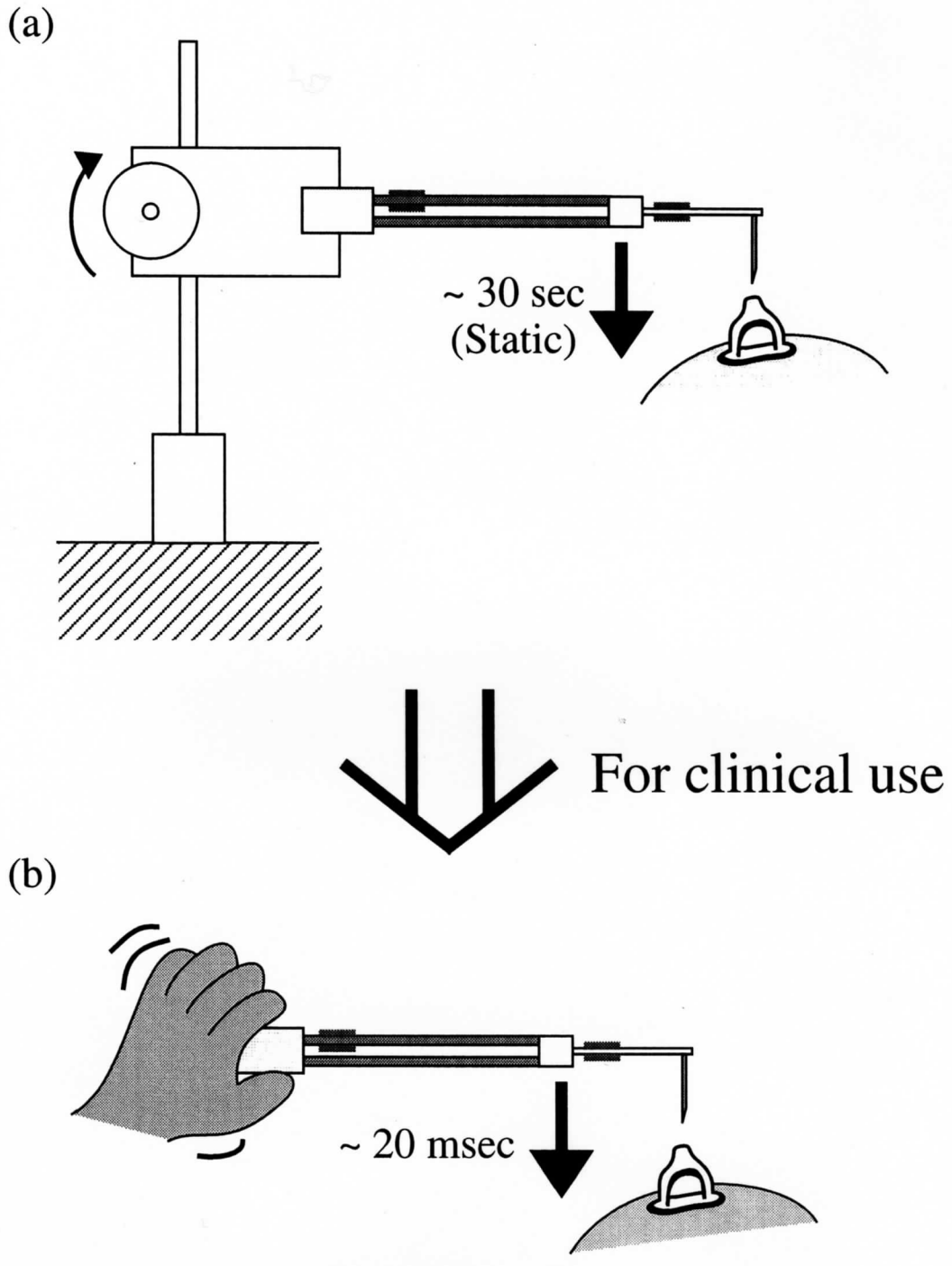

Fig. 3.12. Ways of holding the sensor. (a) The sensor was supported by a micro-manipulator. Measurement was done without noise caused by environmental vibration and took about 30 sec. (b) The sensor was held by hand simulating its use in surgery. Hand trembling sometimes affected the measurement.

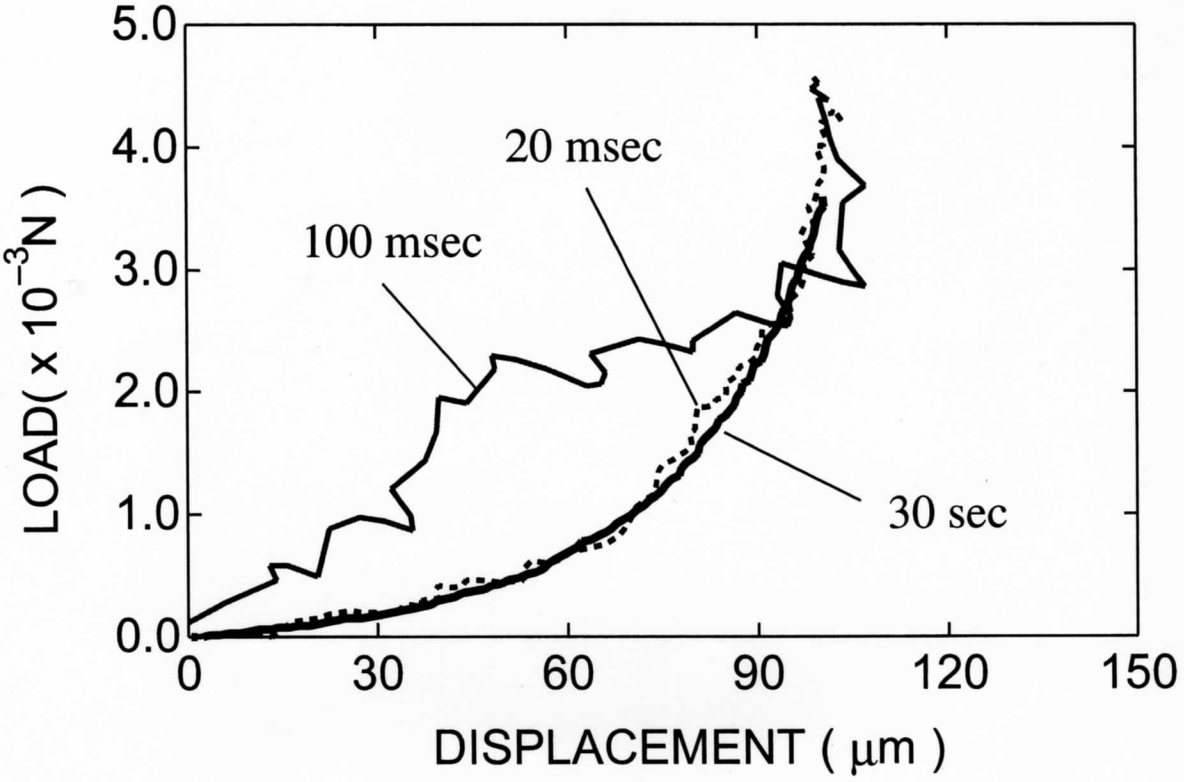

Fig. 3.13. Relationship between the load and displacement of the normal stapes in a guinea pig with the sensor supported by micromanipulator and held by hand. The measurement with the micromanipulator took 30 sec and was considered to be a static measurement. On the other hand, the measurement time when the sensor was held by hand were 100 msec or 20 msec. The result obtained within 100 msec included the noise resulting from hand trembling. However, the result obtained within 20 msec was similar to that of the static measurement.

Table 3.1. Specifications of a force sensors for the measurement of stapes mobility of a human.

Specifications	Necessary conditions
Rated force ($\times 10^{-3}$N)	50
Accuracy ($\times 10^{-3}$N)	$\pm$0.2
Allowable temperature range (℃)	20 - 40
Top view size (mm)	2.1×2.1

Table 3.2. Specifications of an actuator for the measurement of stapes mobility of a human.

Specifications	Necessary conditions
Maximum displacement (μm)	200
Displacement accuracy (μm)	1
Maximum force ($\times 10^{-3}$N)	50
Allowable frequency (Hz)	10
Allowable temperature range (℃)	20 - 40

(a)

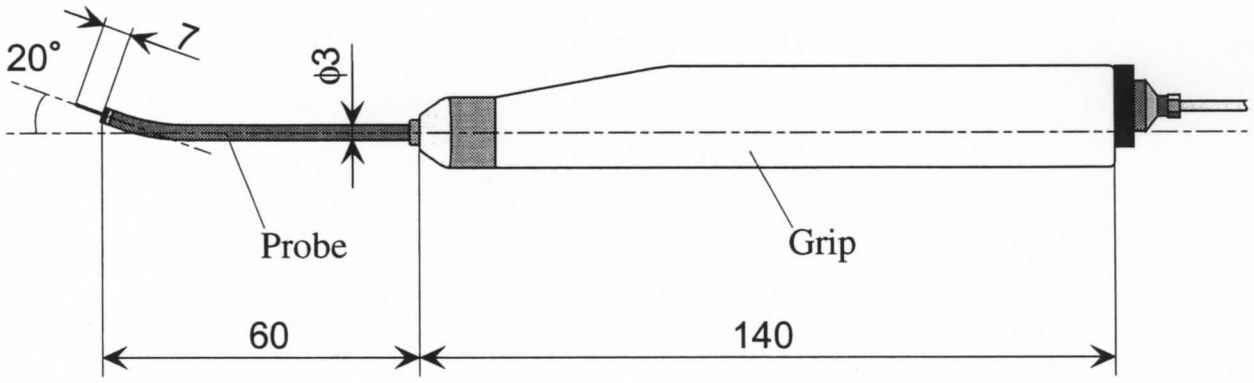

(b)

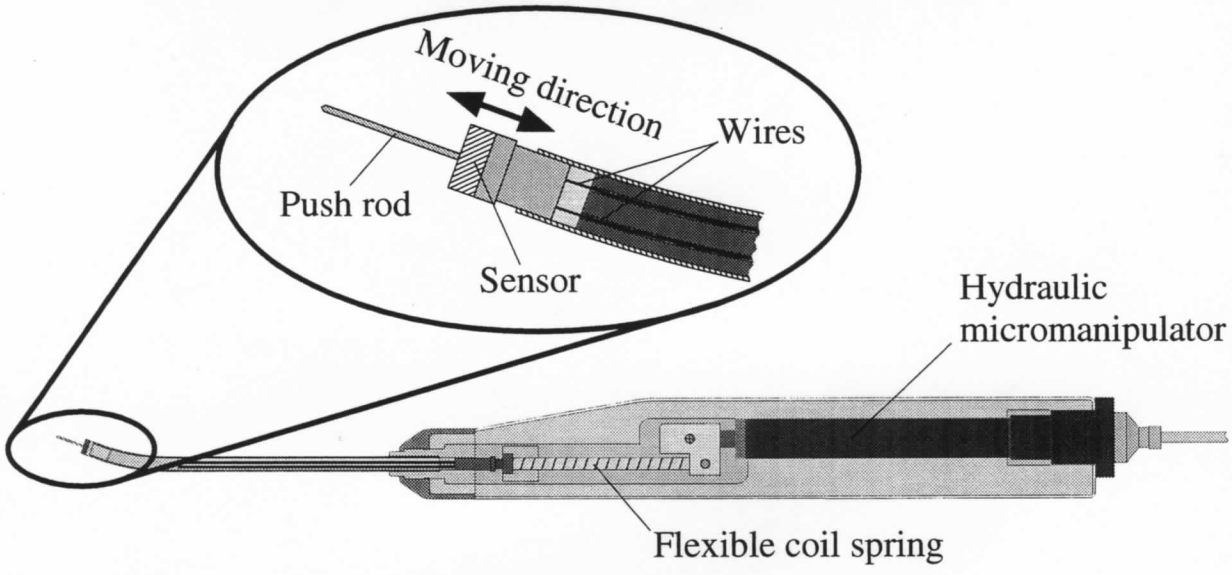

Fig. 3.14. Schematic of a newly designed apparatus for measuring the stapes mobility in humans. (a) Outside. (b) Inside. A force sensor with a push rod is installed in the tip of the apparatus, and connected to a hydraulic micromanipulator which is used as an actuator through a flexible coil spring and wires. The apparatus is designed for practical use in the surgery. Units in millimeters (mm).

(a)

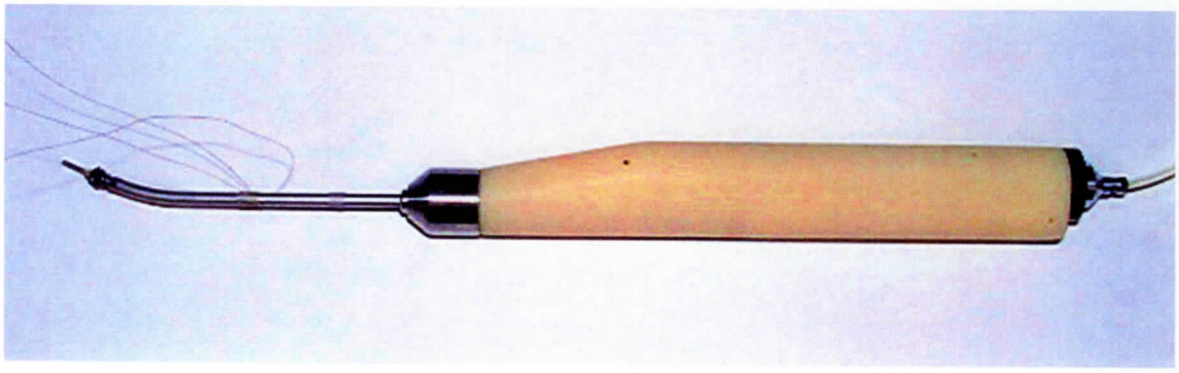

(b)

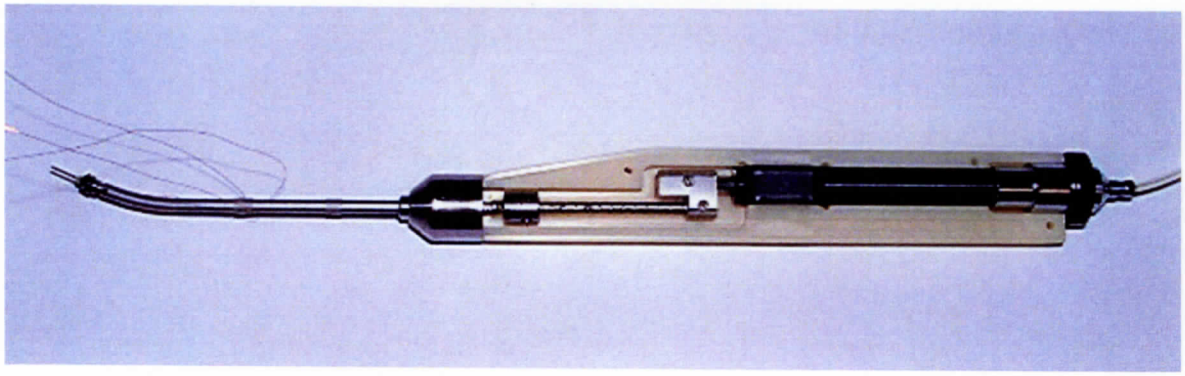

Fig. 3.15. Photographs of a newly designed apparatus for measuring stapes mobility in humans. (a) External unit. (b) Internal unit.

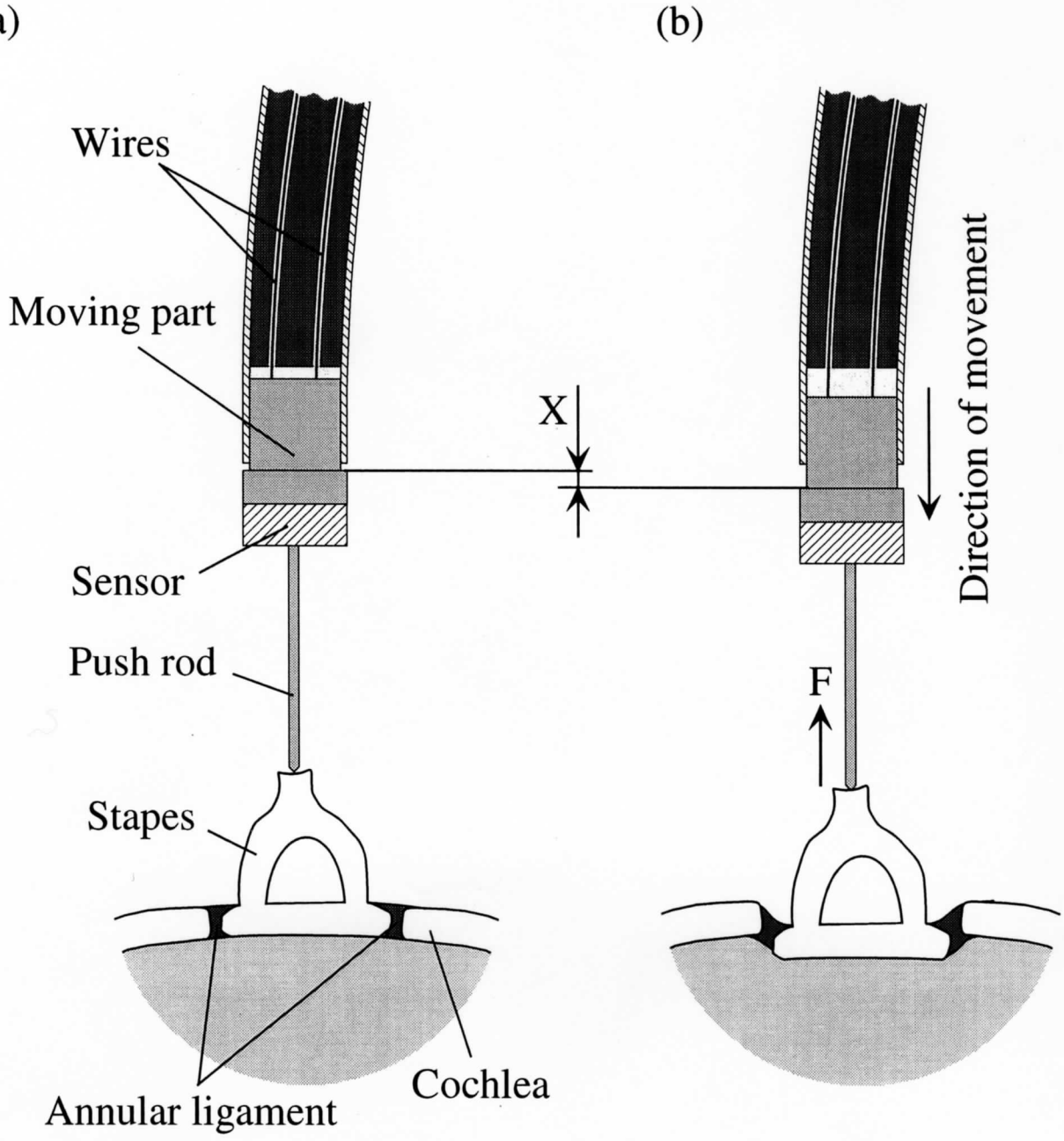

Fig. 3.16. Principle of measurement. (a) Before pushing the stapes. (b) While pushing the stapes. F is the reaction force from the stapes. When a load is applied to the sensor, deflection of the sensor diaphragm occurs. However, the stiffness of the sensor is sufficiently greater than that of the stapes and the deflection is negligible. Therefore, the stapes displacement is considered to be equal to the displacement of the moving part (X) which is driven by the actuator.

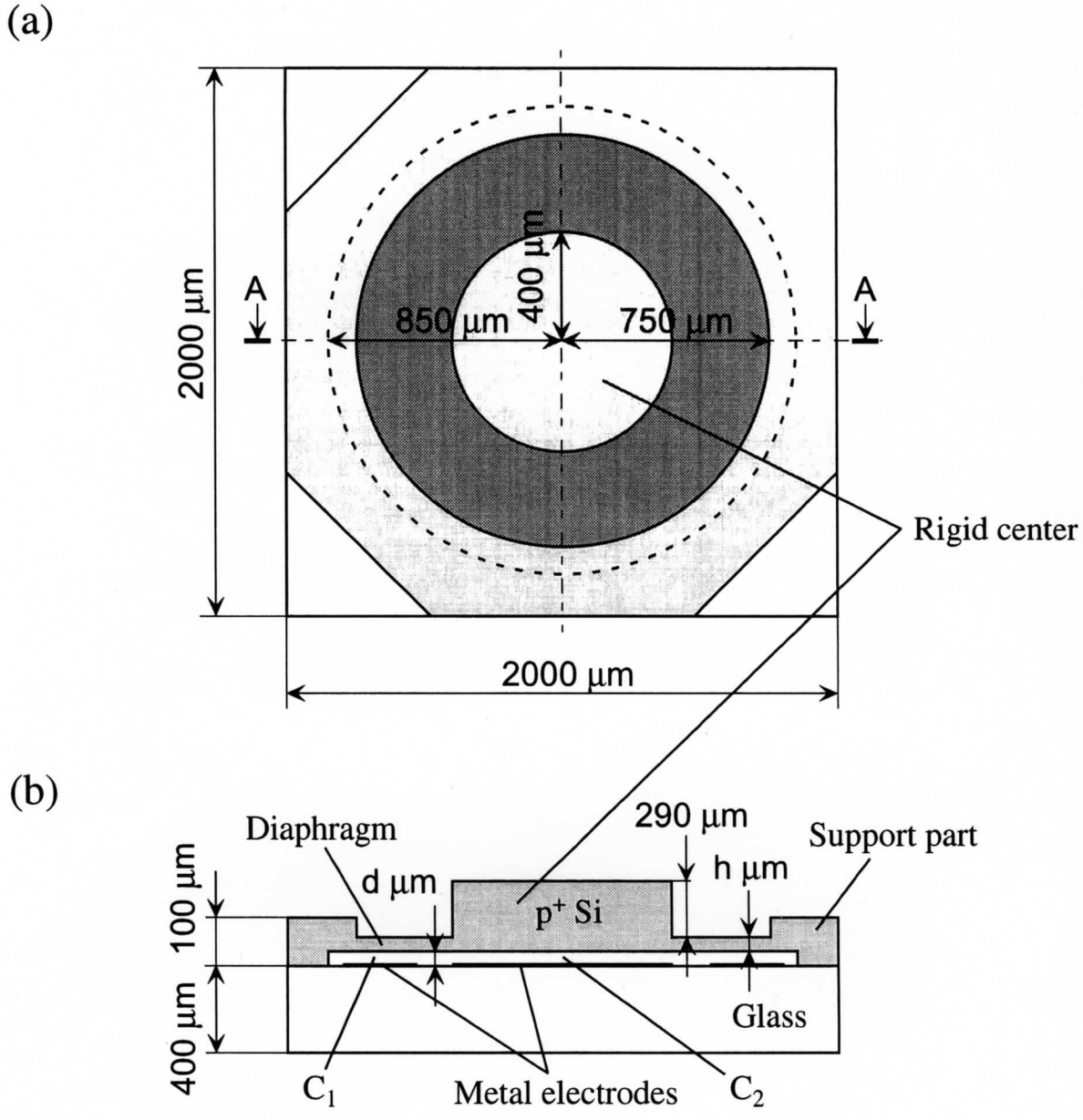

Fig. 3.17. Structure of the capacitive force sensor designed in this study. (a) Top view. (b) Cross section view AA. The sensor has two capacitors C_1 and C_2, which have same capacitances when the diaphragm is unloaded. The C_2 is changed by the load, however C_1 is unchanged. Difference between these capacitances is detected using a diode bridge circuit.

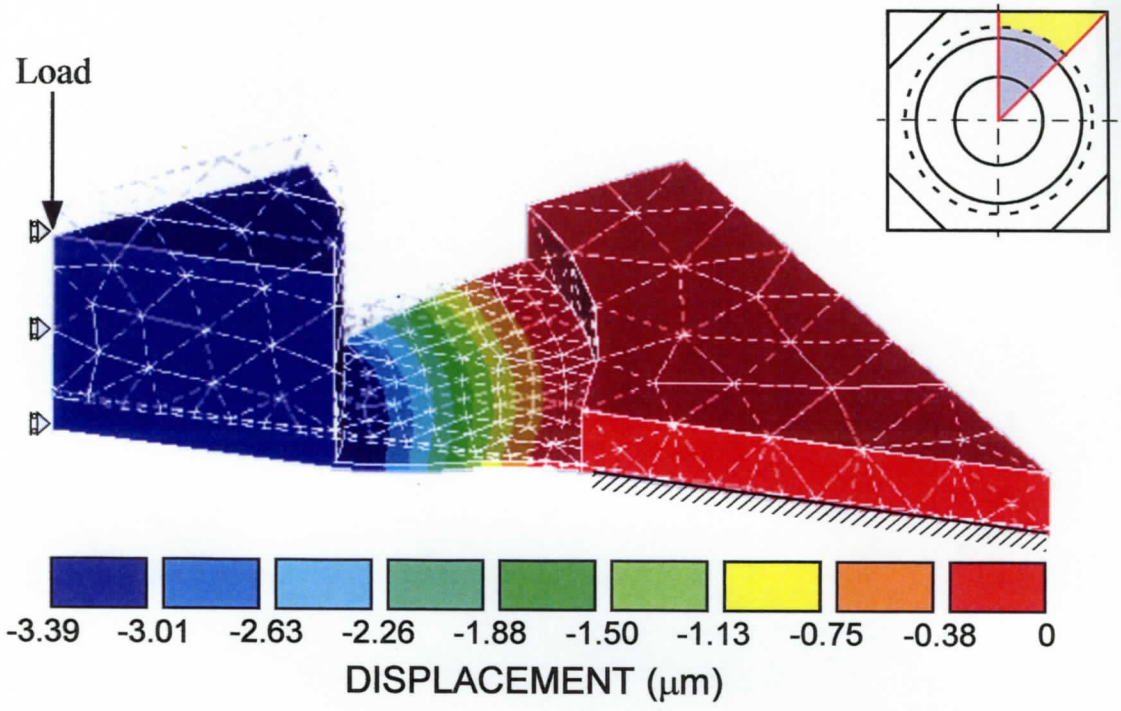

Fig. 3.18. Results of analysis of the loaded force sensor by computer simulation using the finite element method program (ANSYS). The main figure represents the gray and yellow areas of the upper right figure. The boundary condition is as follows: ▨, complete fixation; ▷, fixation which leaves one degree of freedom in the vertical direction; red line in the upper right figure, mirror symmetry; yellow area in the upper right figure, complete fixation area. The applied load in the simulation was 50×10^{-3} N. The height of the diaphragm, and the gap between the diaphragm and electrode were set at 10 μm and 4 μm, respectively.

Silicon process

1. Wet oxidation

p+ Si, t=300 μm

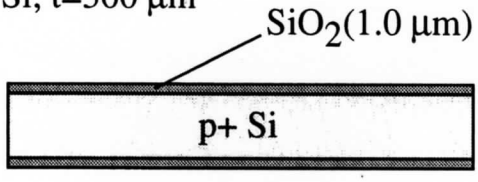

2. TMAH etching

3. Reactive ion etching (RIE)

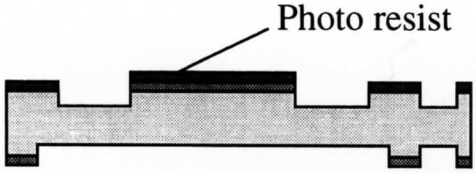

4. Reactive ion etching (RIE)

Glass process

5. Al sputtering

Pyrex grass, t=300 μm

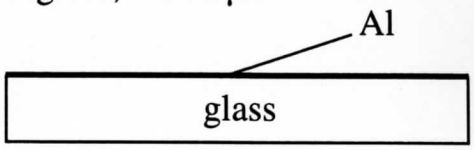

6. Metal electrode patterning

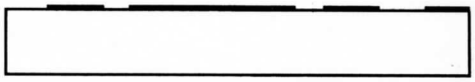

Assembly process

7. Anodic bonding, dicing and wiring

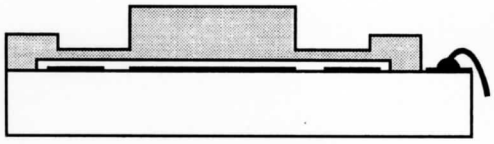

Fig. 3.19. Fabrication process of the sensor. The sensor is made from a 300-μm thick p^+ silicon wafer and a 300-μm-thick piece of pyrex glass.

(a)

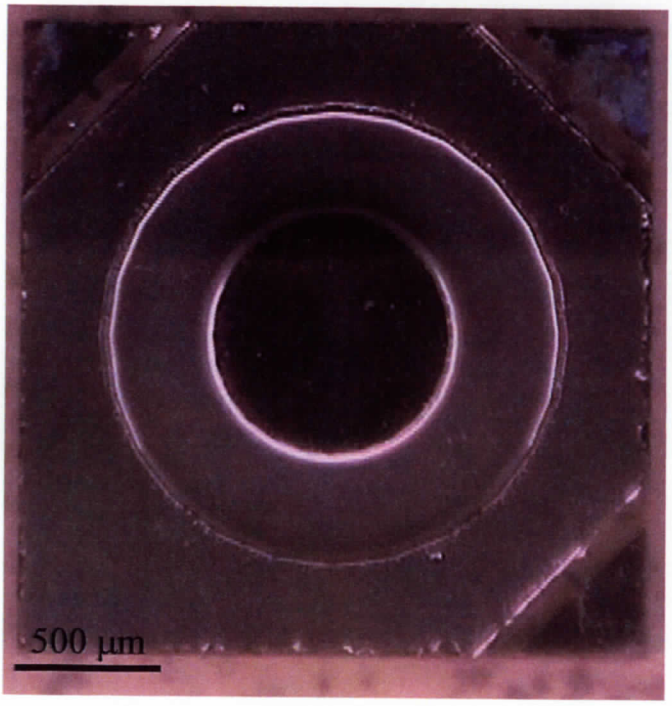

(b)

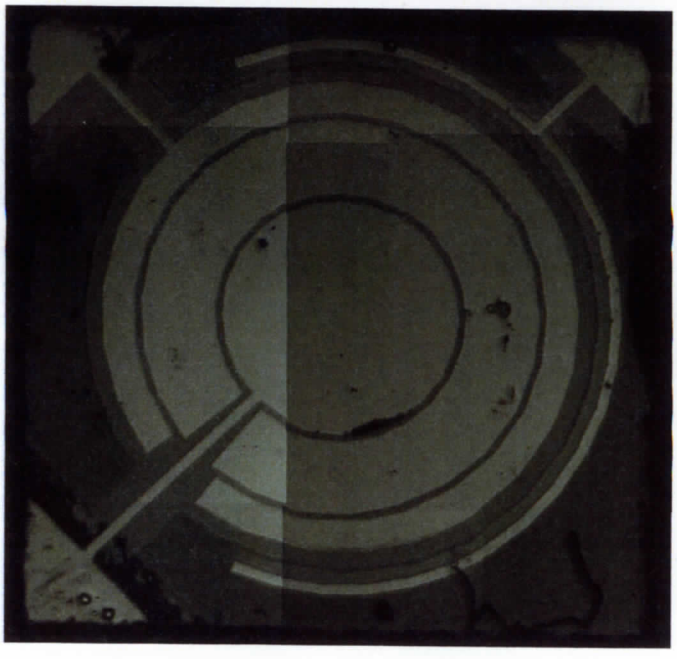

Fig. 3.20. Photograph of the force sensor. (a) Top view. (b) Back view. The top view of the force sensor is 2 by 2 mm.

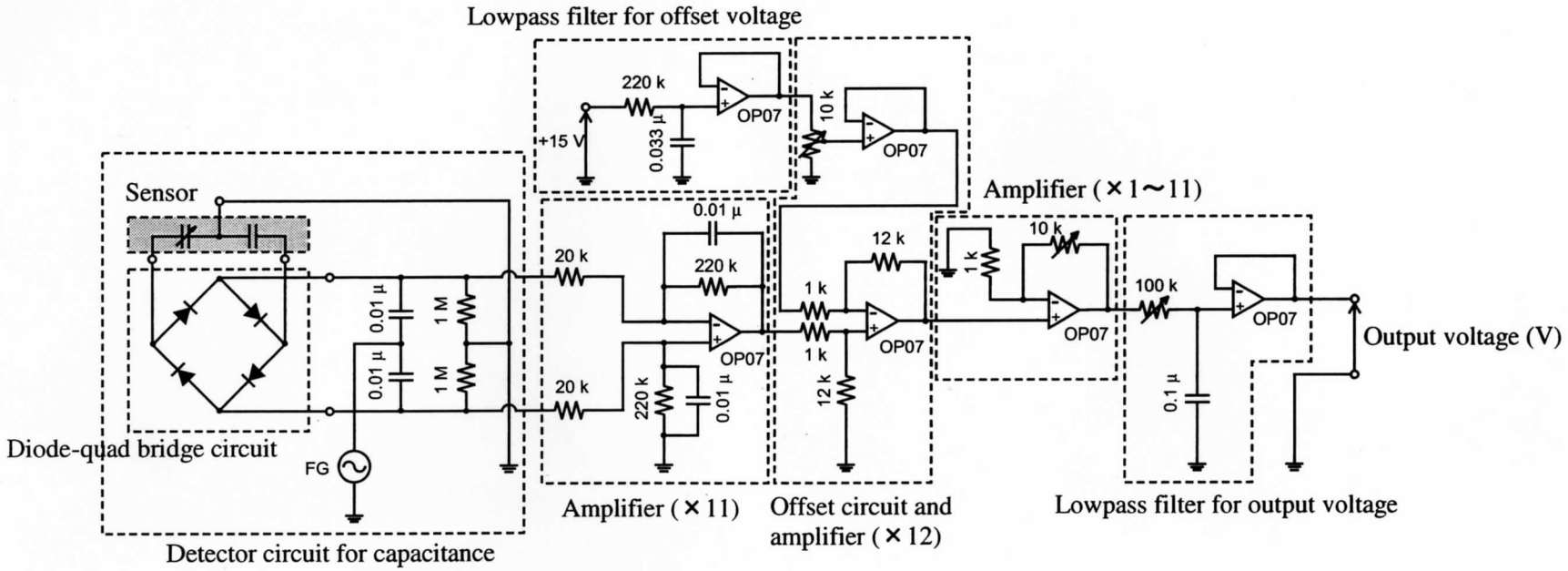

Fig. 3.21. Detector for capacitance and amplifier circuit. The sensor is represented as the capacitors in the gray area. The output voltage is stored in a computer through an A/D board.

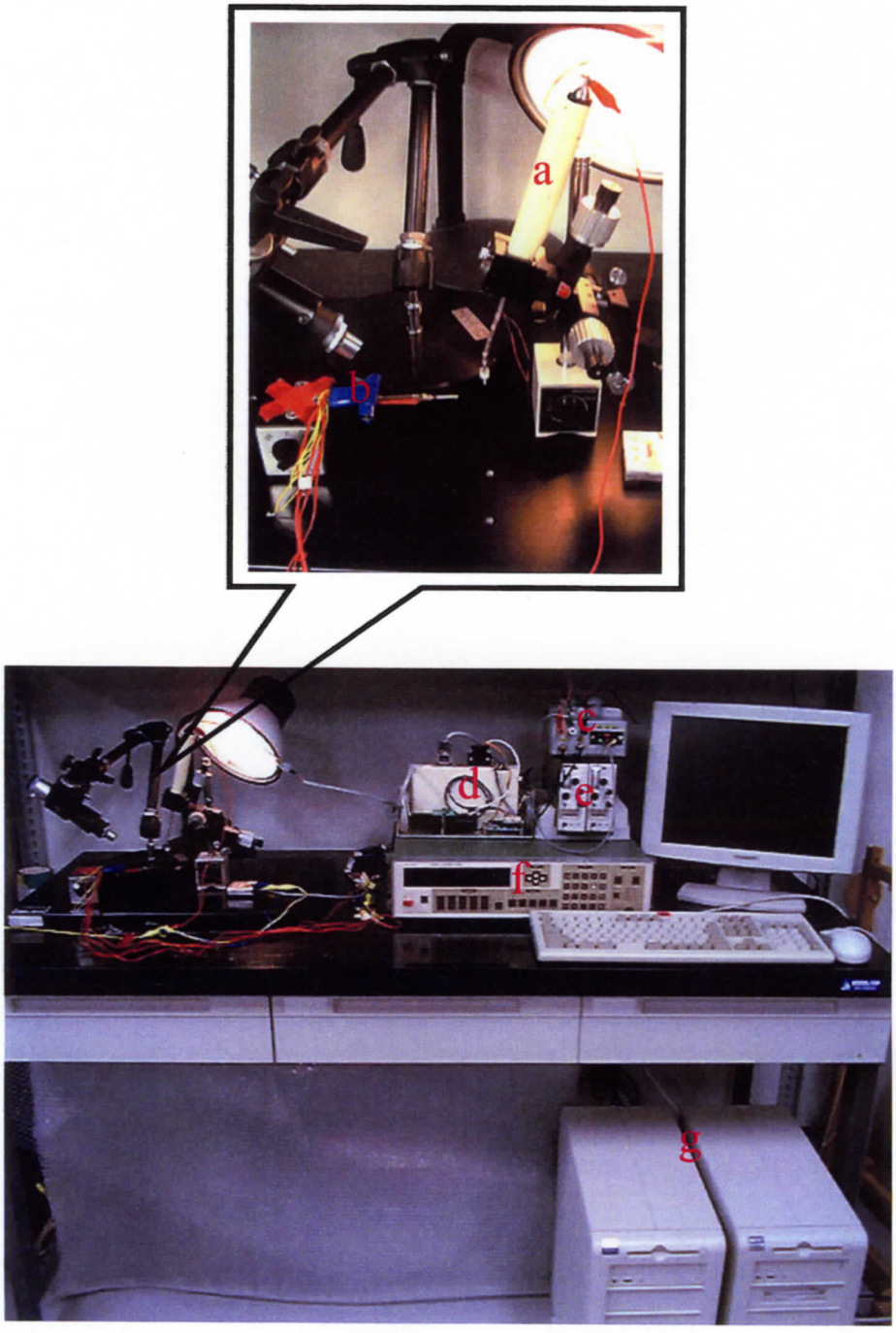

Fig. 3.22. Photographs of measurement system using the apparatus. a, apparatus; b, force sensor used in calibration; c, detector and amplifier circuit for the signal from the apparatus and DC $\pm$15 V battery; d, control unit for the actuator installed into the apparatus; e, amplifier for the simple sensor; f, function generator; g, computers.

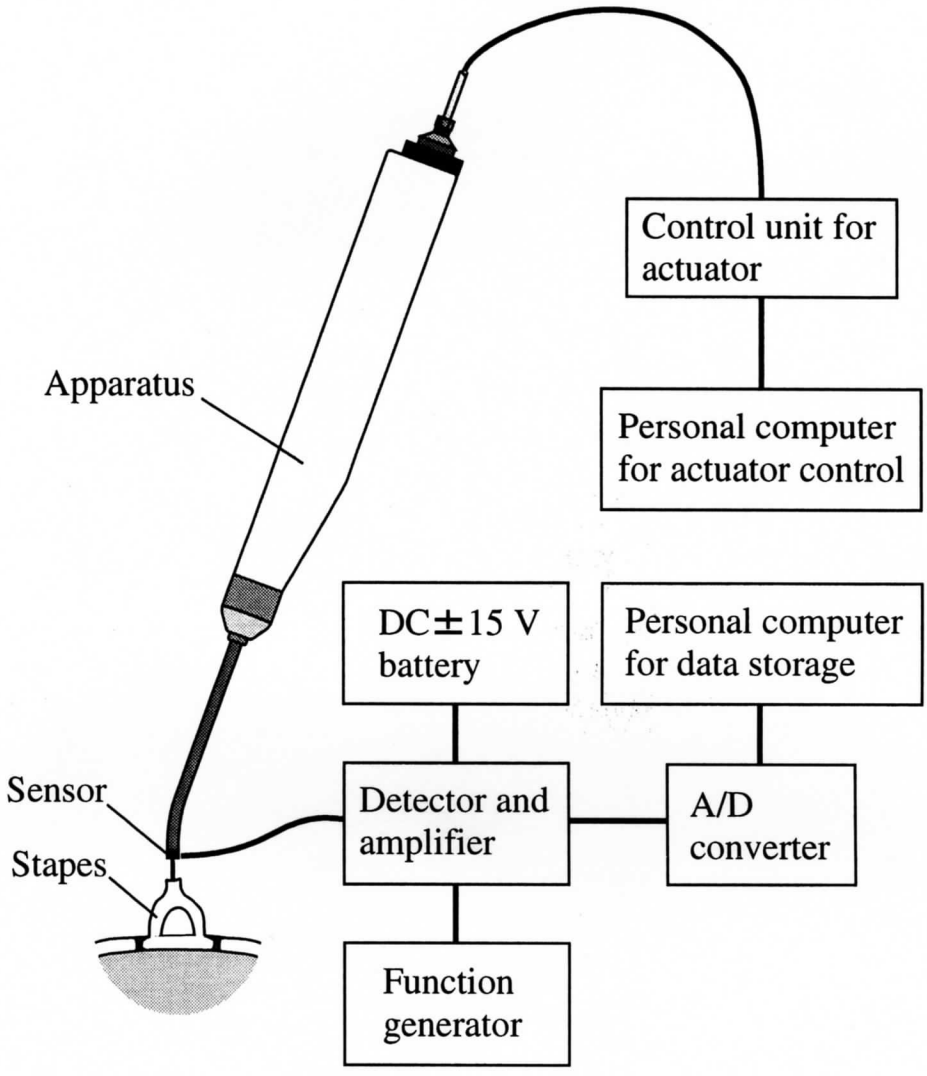

Fig. 3.23. Block diagram of the measurement system of stapes mobility using the apparatus.

Chapter 4. Evaluation and modification of the apparatus

4.1. Method of evaluation

4.1.1. Calibration

The relationship between the output voltage detected by the sensor and the load was measured to obtain the calibration curve. Figure 4.1 is a schematic of calibration measurement. The simple sensor (Fig. 3.1), which had already been calibrated, was pushed by the new apparatus to detect the load. Here, the point which the new apparatus pushed was just behind of the needle which was placed at the end of the beam of the simple sensor. The new apparatus was mounted on the manipulator, and manipulated so that the push rod was put in a vertical position against the simple sensor. Then, the actuator (hydraulic micromanipulator) installed in the new apparatus was turned on, and the sensor and push rod were moved downward. If the push rod touched the simple sensor, the output voltages which were detected by the simple sensor and new apparatus were stored in the computer through an A/D board. The calibration measurements were done semi-statically. The measurement parameters were set as follows. The pushing velocity of the actuator installed in the new apparatus was 650 μm/sec, the moving displacement of the actuator was 250 μm and the sampling frequency of A/D board was 500 Hz. The measurement took about 0.4 sec.

4.1.2. Materials and preparation

Guinea pigs weighing between 0.20 to 0.26 kg (postnatal age 2-3 weeks) were examined in order to evaluate the new apparatus. Figure 3.5 shows a guinea pig used

in the evaluation measurement. The guinea pigs were decapitated and the temporal bones were removed. After opening the bulla, the tympanic membrane, malleus, incus, lateral wall of the middle-ear cavity and a part of the mastoid were removed. The temporal bone was fixed on clay rigidly so that the face of the stapes footplate turned to upward. A small quantity of physiological saline was sometimes applied to prevent drying.

4.1.3. Measurement for evaluation

The relationship between the load and displacement of normal and artificially fixed stapes in a temporal bone of a guinea pig was measured to evaluate the new apparatus. The new apparatus was mounted on the manipulator, and manipulated so that the push rod was located near the stapes head and was vertical against the stapes footplate (Fig. 4.2). Then, the actuator (hydraulic micromanipulator) installed in the new apparatus was driven statically. If the push rod touched the stapes head, the evaluation measurement was started according to principle of measurement (3.2.3). After the measurement of the normal stapes mobility, the stapes was artificially fixed with one drop (about 3×10^{-6} ml) or two drops (about 6×10^{-6} ml) of alkyl-α-cyanoacrilate glue. Such glue was applied to the footplate and the annular ligament. The fixed stapes mobility was also measured with the new apparatus. All the measurements were done semi-statically. The measurement parameters were set as follows, the pushing velocity of the actuator installed into the new apparatus was 650 μm/sec, the moving displacement of the actuator was 150 μm and the sampling frequency of the A/D board was 500 Hz. The measurement took about 0.23 sec.

4.2. Modification

The push rod, which is attached to the sensor, is necessary for improving visibility, if the apparatus is used in the surgery. However, the existence of the push rod was thought to have caused the noise in the measurements.

Figure 4.3 is a schematic of how to assemble the push rod. Firstly, the sensor with a type 'A' push rod, in which a small iron pin was fixed on the rigid-center (Fig. 3.17) of the sensor directly, was evaluated. Figure 4.4 shows the relationship between the output voltage from the sensor and load. There were two kinds of noises, one was periodical noise whose frequency was 250 Hz and the other was irregular noise. Because it was considered that circuit noises caused the periodical noise, the cutoff frequency of the lowpass filter for the output voltage in the circuit was set at 15 Hz, resulting in a decrease of periodical noise.

The irregular noise was thought to be generated by the moments that the diaphragm of the sensor was received from the push rod. To reduce the effect of the moments, a sensor with a type 'B' push rod, in which the iron rod was supported by a rubber cube on the rigid-center of the sensor, was devised (Fig. 4.3 (b)). Figure 4.5 shows the relationship between the output voltage from the sensor and load. Most of the noise was reduced and the relationship was clarified. However, as indicated by the arrow, a slight influence of the moment remained. The output voltage increased nonlinearly with an increase in load. Using the apparatus with the type 'B' push rod, the stapes mobility of the guinea pig was measured *in vitro*. Figure 4.6 shows the relationship between the load and displacement of the normal stapes of a guinea pig. Noise with a frequency of 50 Hz was detected. It was considered that the iron rod received the noise of electric power supply through the stapes which is a part of the

living body. This noise was not evident when using the metals as measurement objects.

To eliminate the noise from the electric power supply, the sensor with a type 'C' push rod was devised (Fig. 4.3 (c)). An iron rod was replaced by a plastic rod. Furthermore, to eliminate the moment noise completely, the rod was supported by two rubber membranes and was not fixed on the rigid-center of the sensor. Also, the rod applied a pre-load to the sensor. Figure 4.7 shows the relationship between the output voltage from the sensor with type 'C' push rod and load. The load increased linearly with an increase in output voltage. Because the sensor was applied pre-load, only the linear region of the output property of the sensor was used. Figure 4.8 shows the relationship between the load and displacement of normal stapes in a guinea pig measured by the apparatus with type 'C' push rod in vitro. The noise which was considered to be caused by the electric power supply was eliminated and a clear line was obtained.

In the following experiment, the apparatus with the type 'C' push rod was used as the final apparatus in this study.

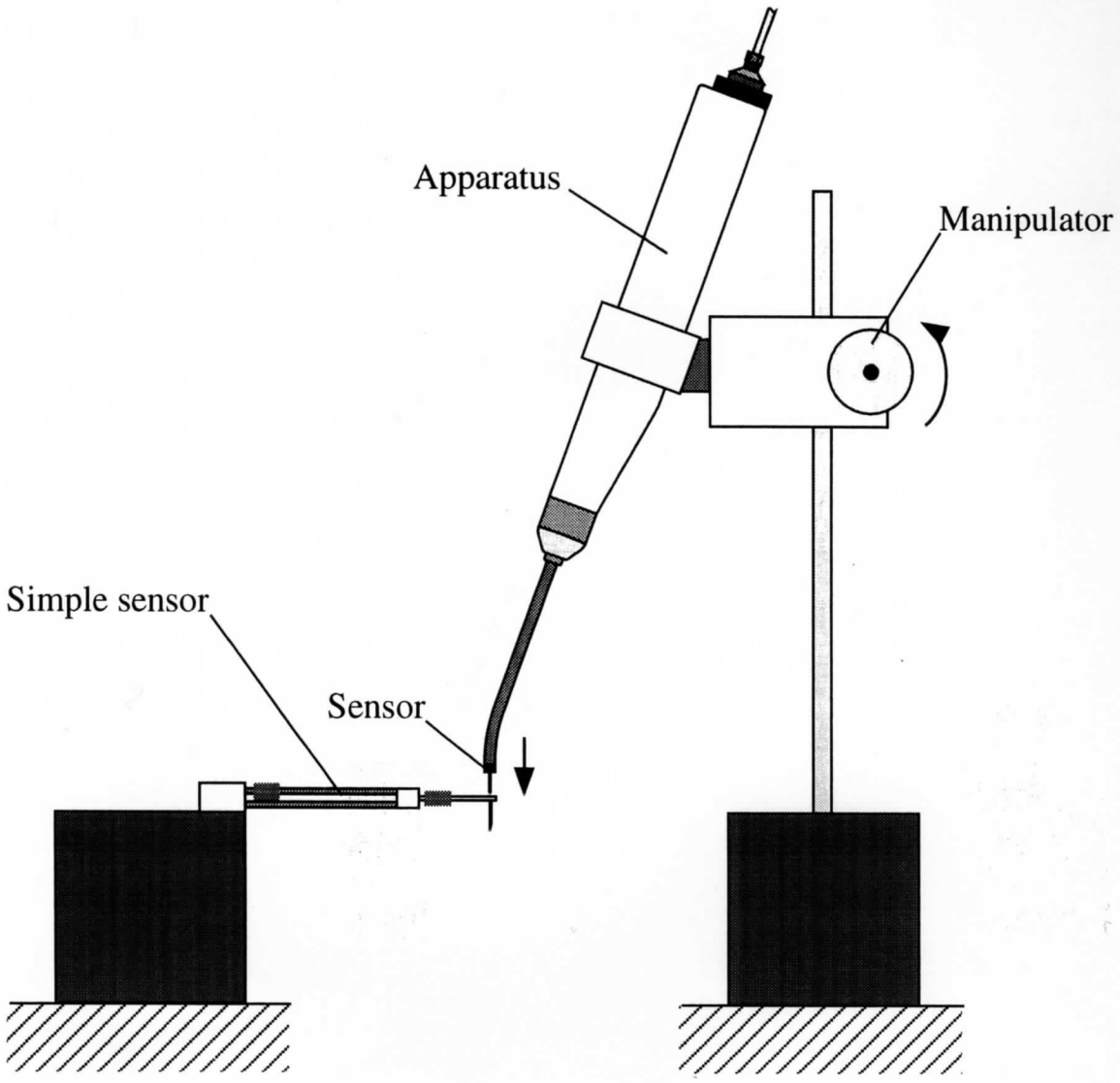

Fig. 4.1. Schematic of calibration. The relationship between the load and the output voltage detected by the sensor of the new apparatus was measured. The simple sensor (Fig. 3.1), which had been already calibrated, was pushed by the new apparatus to detect the load. Here, the point which the new apparatus pushed was just behind of the needle which was placed on the end of the beam of the simple sensor. The new apparatus was mounted on the manipulator, and manipulated so that the push rod was placed near and vertical against the simple sensor. The calibration measurements were done semi-statically. The measurement parameters were set as follows but the measurement using the new apparatus under modification, the pushing velocity of the actuator installed into the new apparatus was 650 mm/sec, the moving displacement of the actuator was 250 mm and the sampling frequency of A/D board was 500 Hz. It took about 0.4 sec in the measurement.

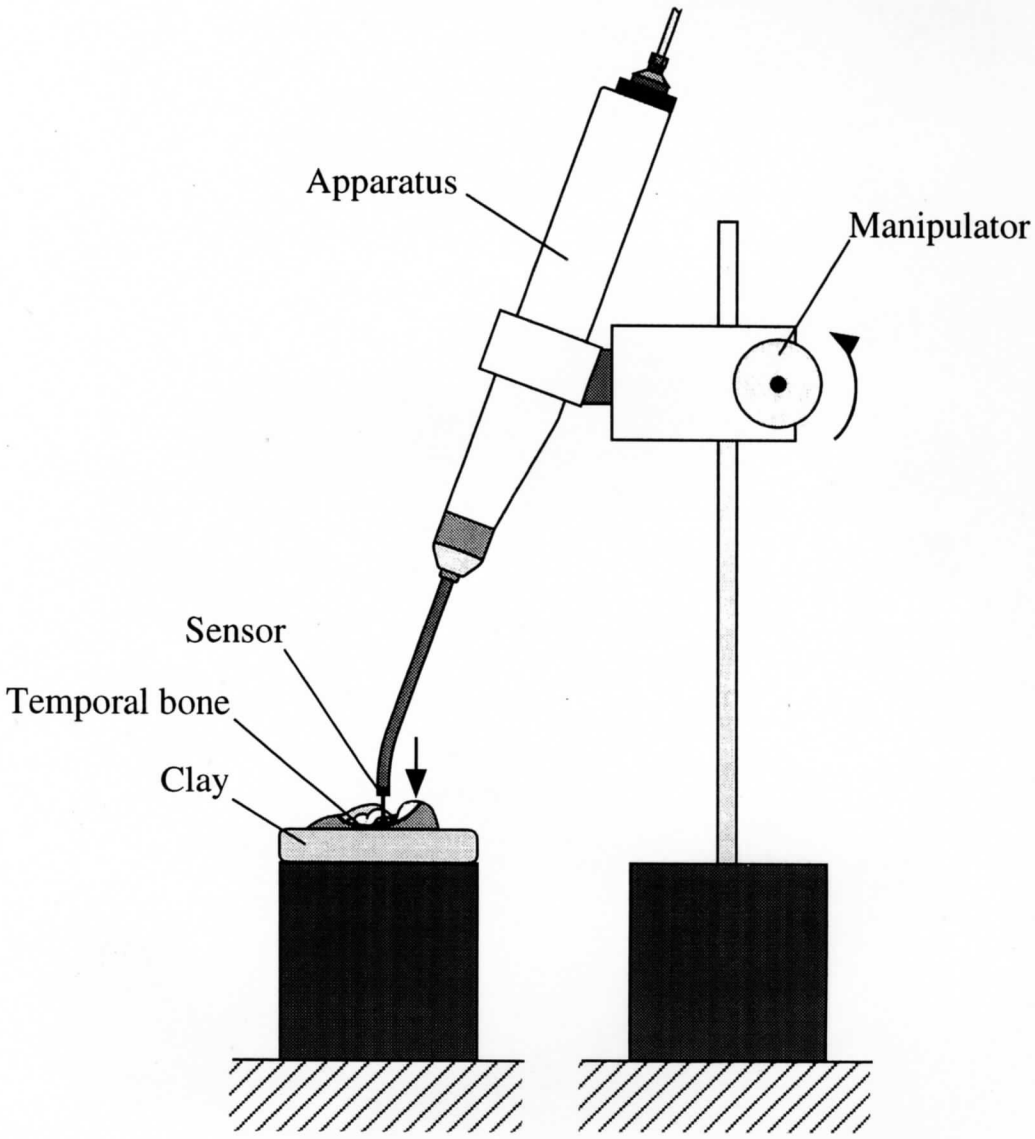

Fig. 4.2. Schematic of measurement. The relationship between the load and displacement of normal and artificially fixed stapes in a temporal bone of a guinea pig was measured. The new apparatus was mounted on the manipulator, and manipulated so that the push rod was put near the stapes head and vertical against the stapes footplate. After the measurement of the normal stapes mobility, the stapes was artificially fixed with one drop (about 3×10^{-6} ml) or two drops (about 6×10^{-6} ml) of alkyl-a-cyanoacrilate glue. The glue was applied to the footplate and the annular ligament. The measurement was done semi-statically. The measurement parameters were set as follows but the measurement using the new apparatus under modification, the pushing velocity of the actuator installed into the new apparatus was 650 mm/sec, the moving displacement of the actuator was 150 mm and the sampling frequency of A/D board was 500 Hz. Measurement took about 0.23 sec.

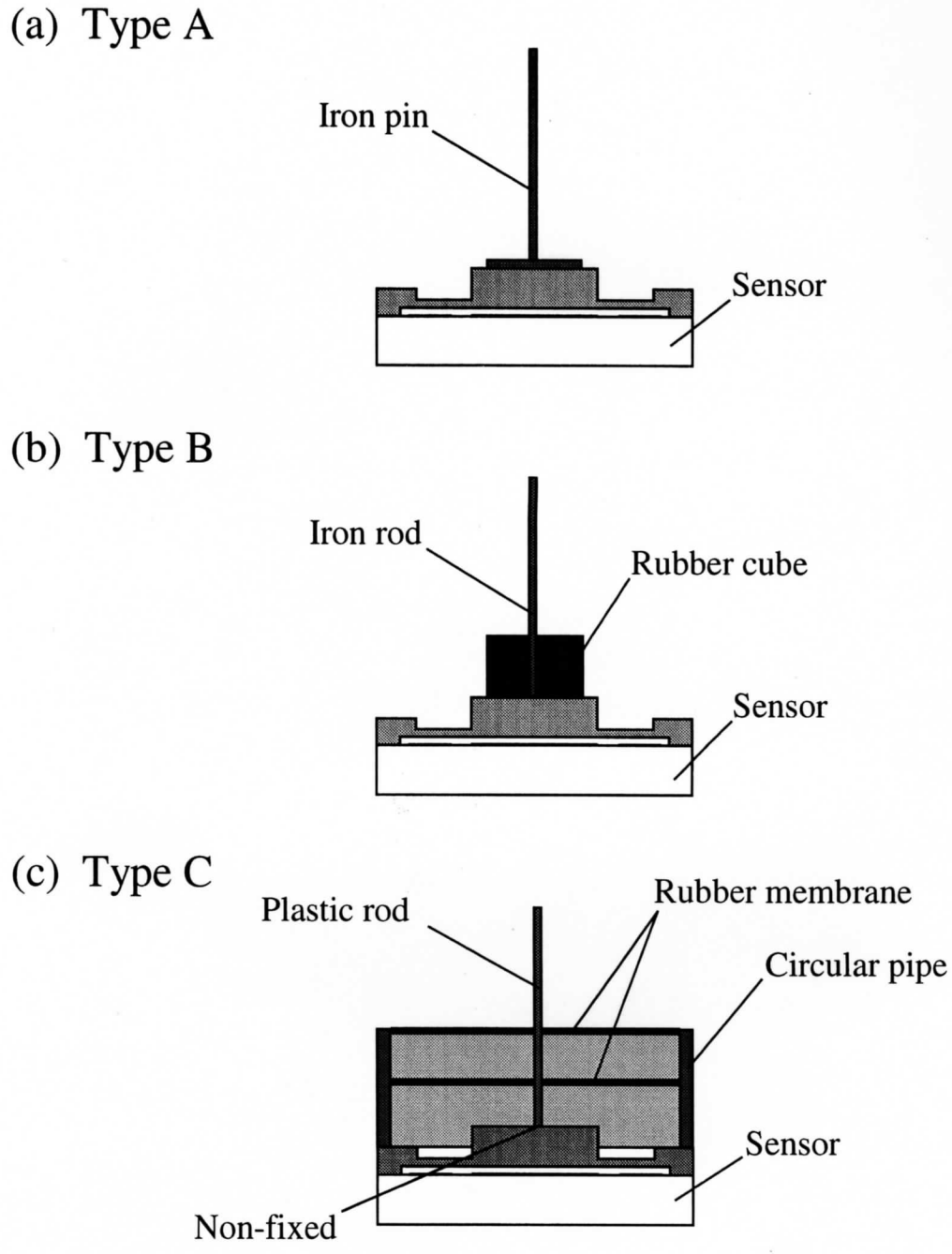

Fig. 4.3. Schematic of how the push rod was assembled. (a) Type A: A small iron pin was glued on the rigid-center of the sensor directly. (b) Type B: A iron rod was supported by a rubber cube on the rigid-center of the sensor. (c) Type C: A plastic rod is supported by two rubber membranes without the rod being glued onto the rigid-center of the sensor, and the rod applied pre-load to the sensor.

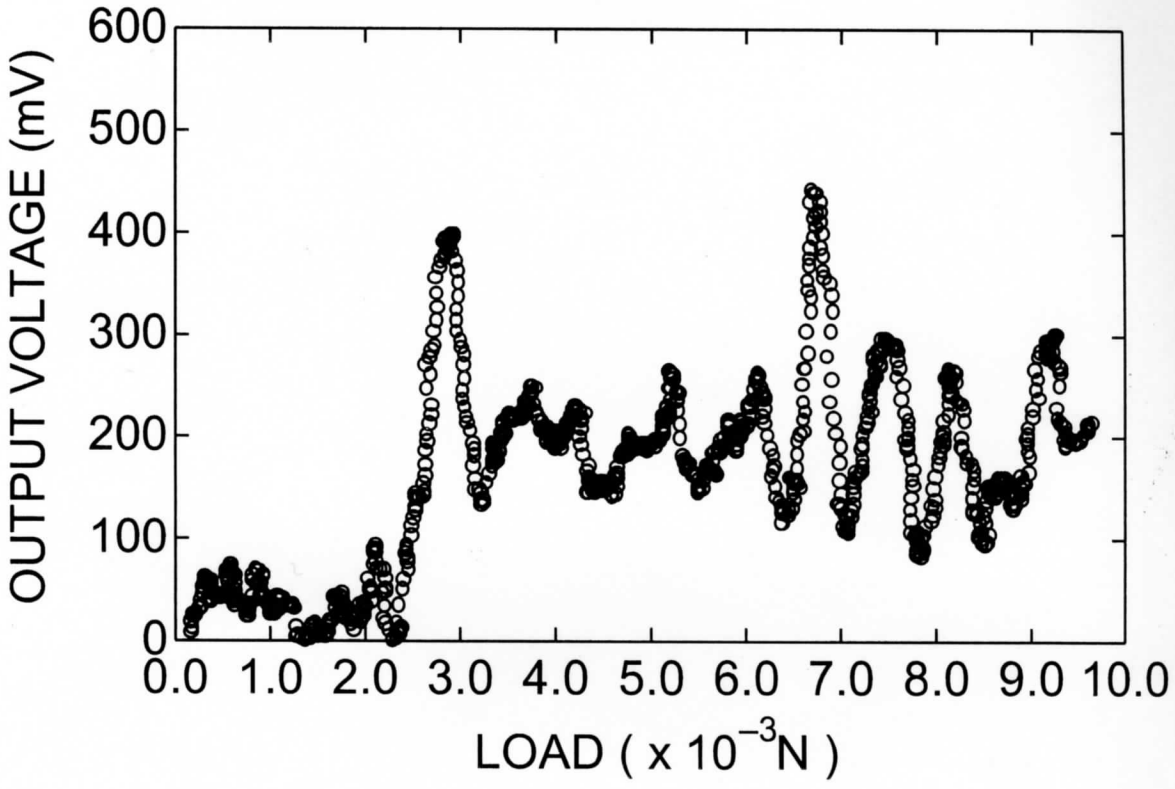

Fig. 4.4. Relationship between the output voltage form the sensor and load with type A push rod. The apparatus was mounted on the manipulator. The simple sensor (Fig. 3.1), which had already been calibrated, was used for the measurement. The measurement was done semi-statically. The pushing velocity of the actuator installed into the new apparatus was 250 μm/sec, the moving displacement of the actuator was 250 μm and the sampling frequency of A/D board was 1000 Hz. The measurement took 1.0 sec.

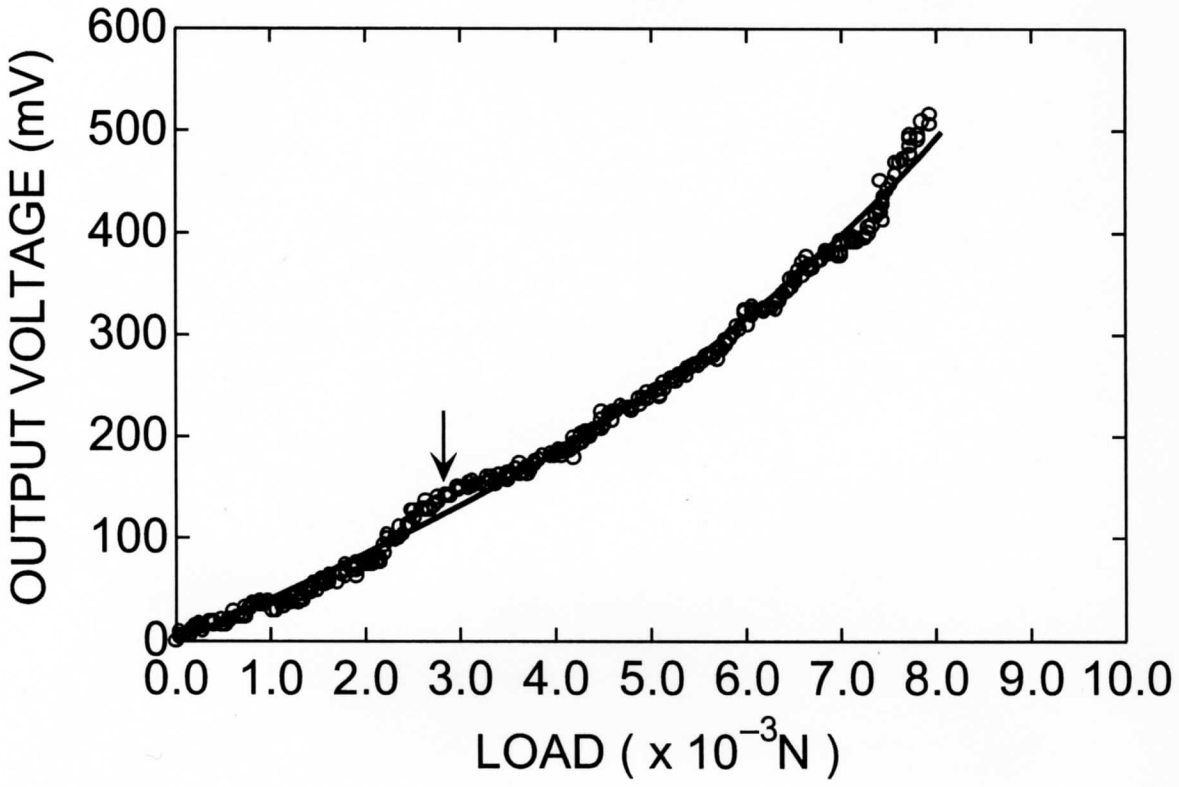

Fig. 4.5. Relationship between the output voltage from the sensor and load with type B push rod. The apparatus was mounted on the manipulator. The simple sensor (Fig. 3.1), which had already been calibrated, was used for the measurement. The measurement was done semi-statically. The pushing velocity of the actuator installed in the new apparatus was 8 μm/sec, the moving displacement of the actuator was 250 μm and the sampling frequency of A/D board was 10 Hz. The measurement took 30 sec. The arrow indicates a slight influence of moment.

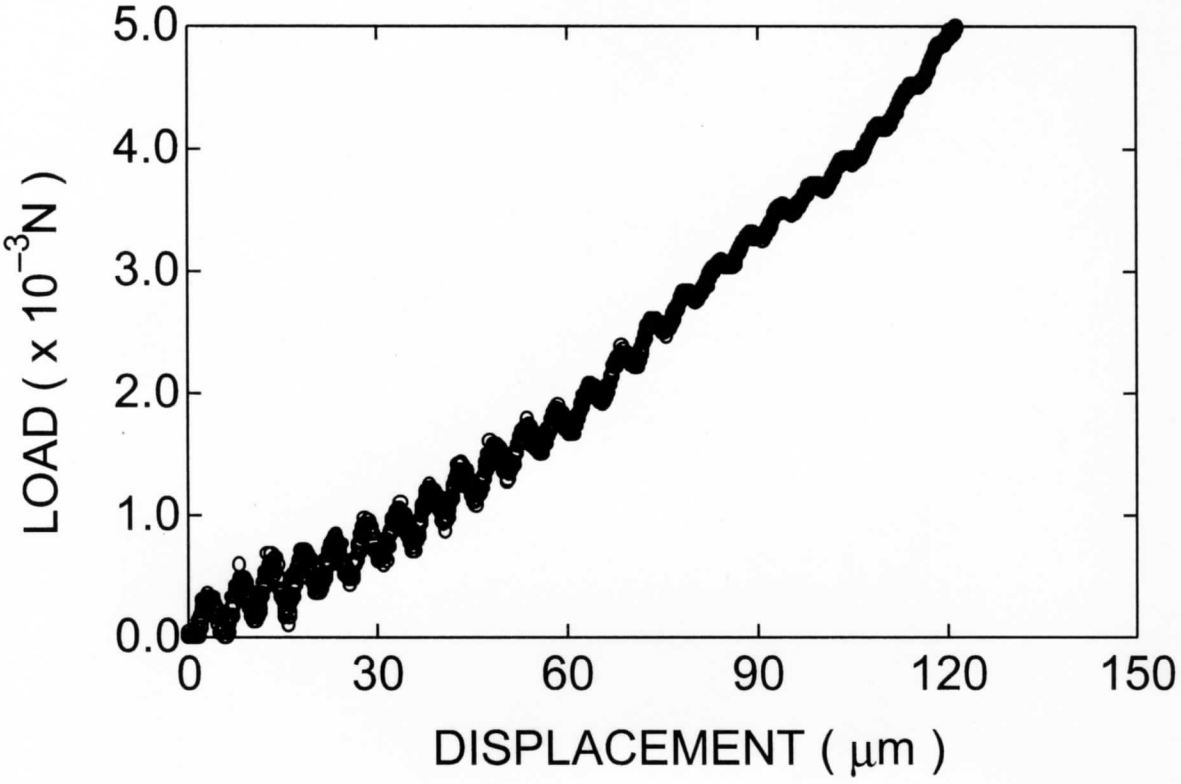

Fig. 4.6. Relationship between the load and displacement of normal stapes in a guinea pig measured by the apparatus with the type B push rod. The apparatus was mounted on the manipulator. A temporal bone of a guinea pig was used for the measurement. The measurement was done semi-statically. The pushing velocity of the actuator installed into the new apparatus was 250 μm/sec, the moving displacement of the actuator was 150 μm and the sampling frequency of A/D board was 300 Hz. It took 0.6 sec in the measurement.

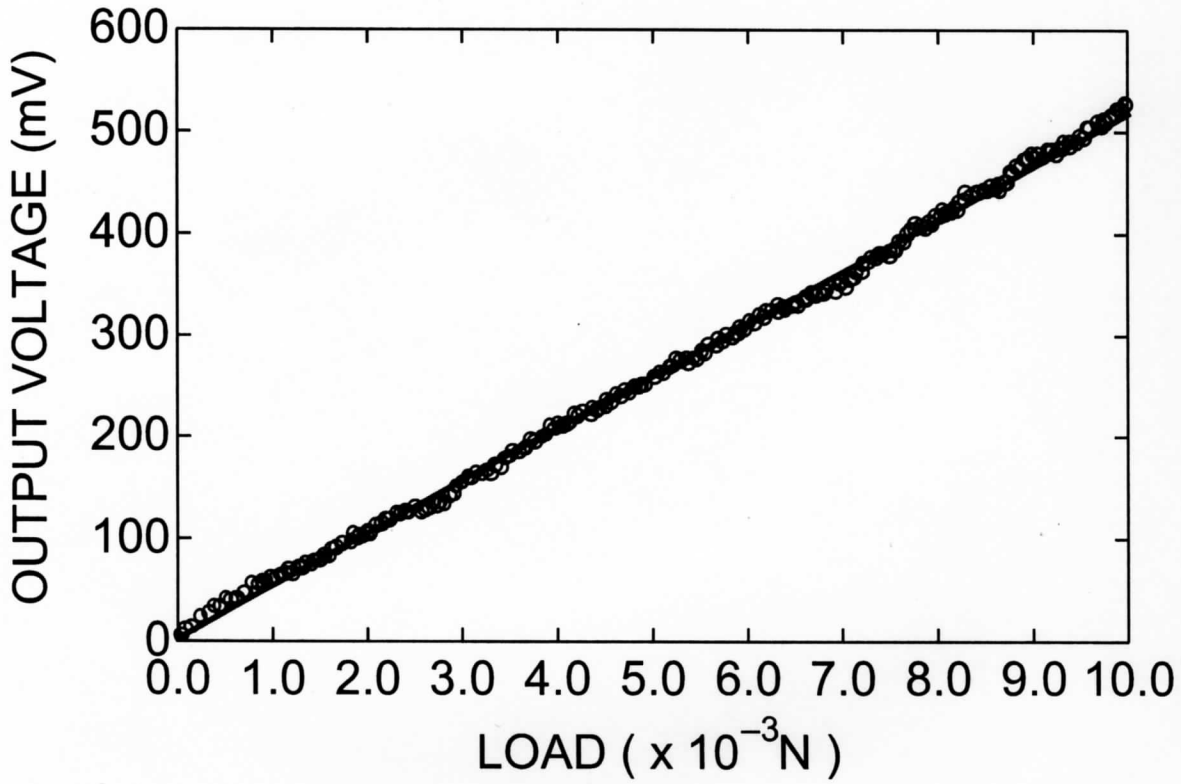

Fig. 4.7. Relationship between the output voltage form the sensor and load with type C push rod. The apparatus was mounted on the manipulator. The simple sensor (Fig. 3.1), which was already calibrated, was used for the measurement. The measurement was done semi-statically. The pushing velocity of the actuator installed into the new apparatus was 650 μm/sec, the moving displacement of the actuator was 250 μm and the sampling frequency of A/D board was 500 Hz. It took 0.38 sec in the measurement.

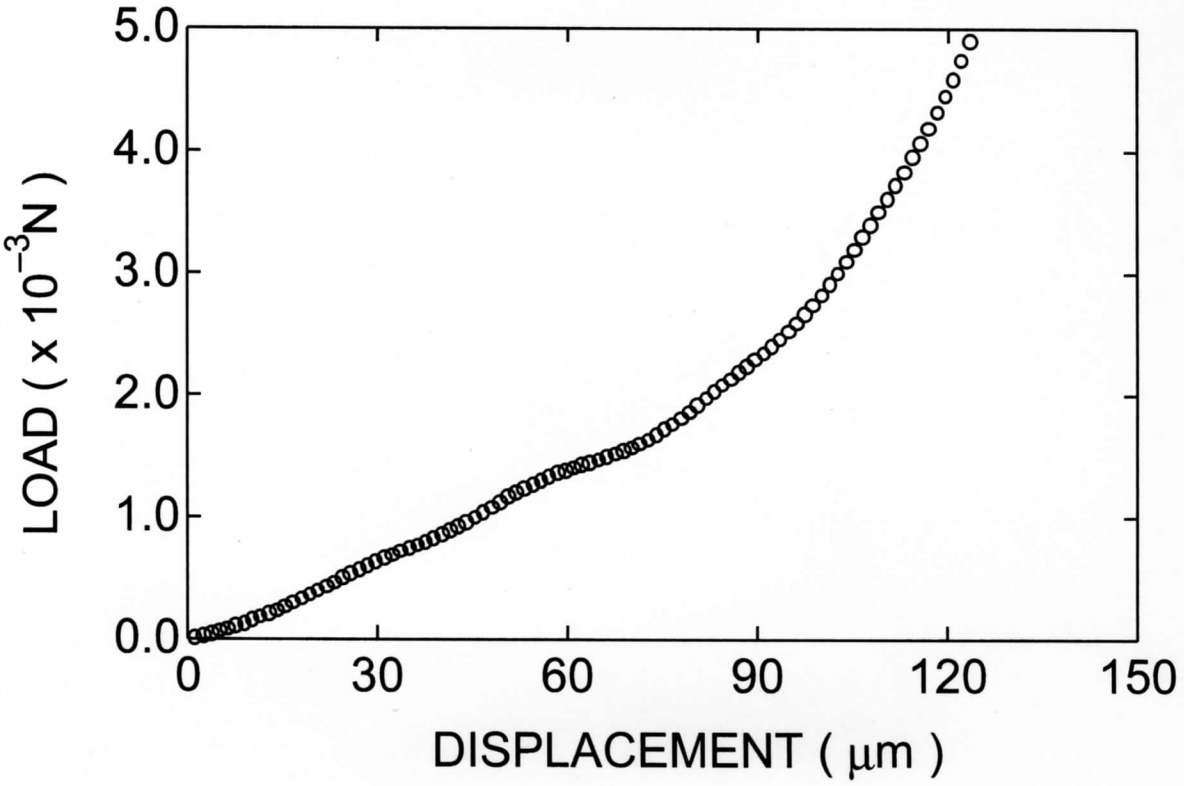

Fig. 4.8. Relationship between the load and displacement of normal stapes in a guinea pig measured by the apparatus with type C push rod. The apparatus was mounted on the manipulator. A temporal bone of a guinea pig was used for the measurement. The measurement was done semi-statically. The pushing velocity of the actuator installed into the new apparatus was 650 μm/sec, the moving displacement of the actuator was 150 μm and the sampling frequency of A/D board was 500 Hz. It took 0.23 sec in the measurement.

Chapter 5. Results

5.1. Mobility of normal stapes

Figure 5.1 shows an example of the relationship between the load and displacement of the normal stapes in a guinea pig measured by the new apparatus. The displacement increased linearly with an increase in load in the small displacement region, but nonlinearly increased in the large displacement region. This tendency corresponds to that measured by the simple sensor in the pilot experiment. The regression line of the relationship between the load and displacement in the region under 1.0×10^{-3} N was computed by the minimum square method, and its slope, i.e., the equivalent stiffness, was used for evaluating stapes mobility in a way similar to the pilot experiment. The equivalent stiffness in Fig. 5.1 was 21 N/m.

The repeatability of stiffness measurement is shown in Fig. 5.2. The equivalent stiffness was measured three times in the same guinea pig. The average of equivalent stiffness was 19.6 N/m, and the standard deviation was 0.8 N/m. The standard deviation was about 4% of the average.

The measurements were performed on 5 ears in 4 guinea pigs. Figure 5.3 (a) shows the relationship between load and displacement in each guinea pig. All the measurement results were found within the hatched areas shown in Fig. 5.3 (b). The average value of the equivalent stiffness obtained from 5 guinea pigs was 17 ± 3 N/m. In these measurements, the correlation coefficients of the regression lines ranged from 0.96 to 0.99.

5.2. Mobility of artificially fixed stapes

Figure 5.4 shows the change of the equivalent stiffness before and after the artificial fixation of the stapes in a guinea pig. When one drop (about 3×10^{-6} ml) of the glue was dripped onto the annular ligament, the equivalent stiffness changed from 19 N/m to 124 N/m, and when two drops (about 6×10^{-6} ml) of the glue were applied, the equivalent stiffness changed to 185 N/m.

The measurements were performed on 5 ears in 4 guinea pigs. All the measurement results of normal stapes were found within the hatched area shown in Fig. 5.5, and those of artificially fixed stapes were found within the gray area. The average equivalent stiffness of all results obtained from the normal and artificially fixed stapes were 17 ± 3 N/m (N = 5) and 151 ± 32 N/m (N = 5), respectively. In these measurements, the correlation coefficients of the regression lines ranged from 0.84 to 0.99.

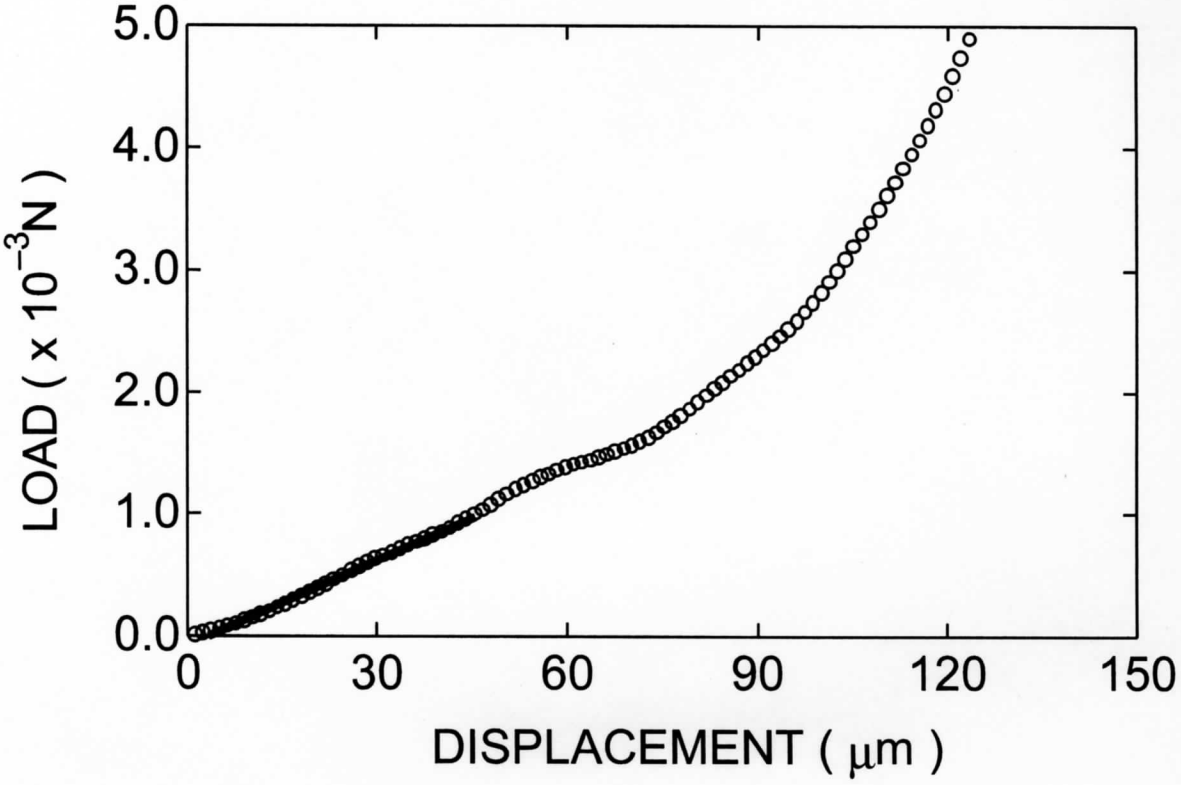

Fig. 5.1. Relationship between the load and displacement of normal stapes in a guinea pig measured by the new apparatus. A temporal bone of a guinea pig was used for the measurement. The measurement was done semi-statically. The pushing velocity of the actuator installed into the new apparatus was 650 μm/sec, the moving displacement of the actuator was 150 μm and the sampling frequency of A/D board was 500 Hz. Measurement took 0.23 sec. The equivalent stiffness 21 N/m was obtained from the regression line, and correlation coefficient was r = 0.99.

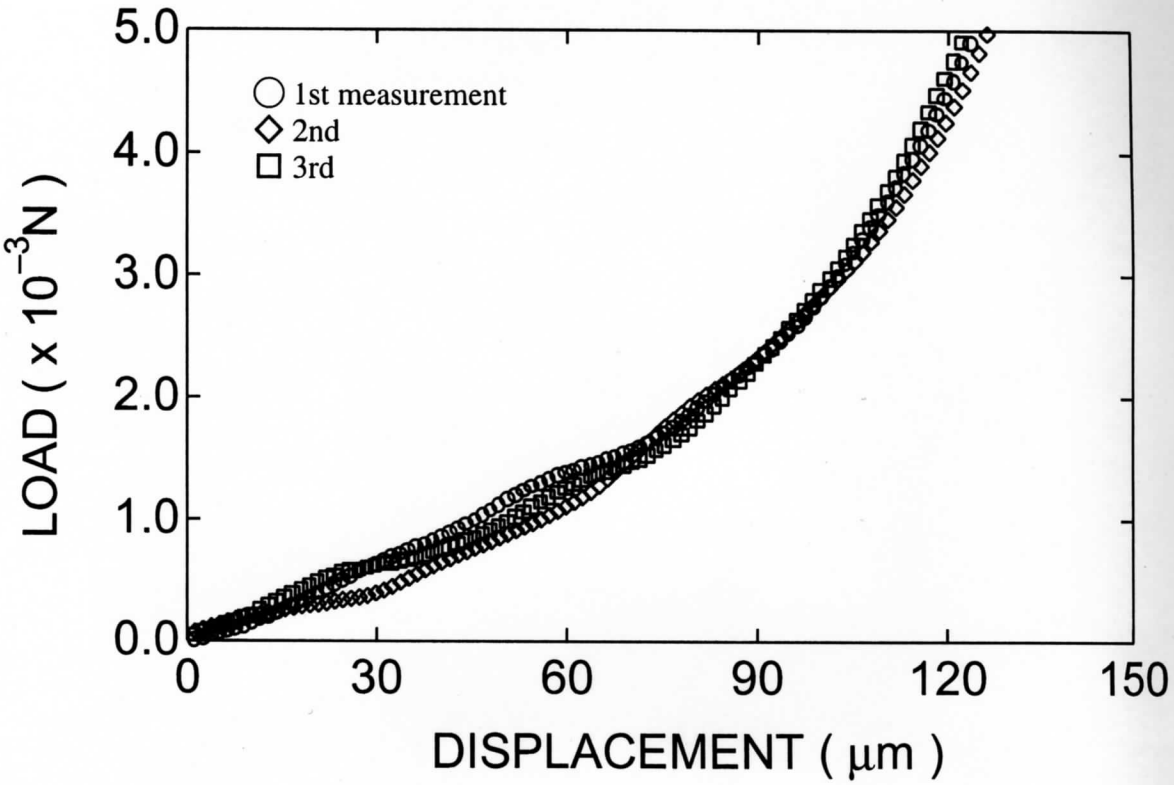

Fig. 5.2. Repeatability of the measurement of normal stapes in a guinea pig using the new apparatus. A temporal bone of a guinea pig was used for the measurements and three measurements were made in one stapes. The measurements were done semi-statically. The pushing velocity of the actuator installed in the new apparatus was 650 μm/sec, the moving displacement of the actuator was 150 μm and the sampling frequency of A/D board was 500 Hz. Measurements took 0.23 sec. The average equivalent stiffness was 19.6±0.8 N/m. The standard deviation was 4.1 % of the average.

(a)

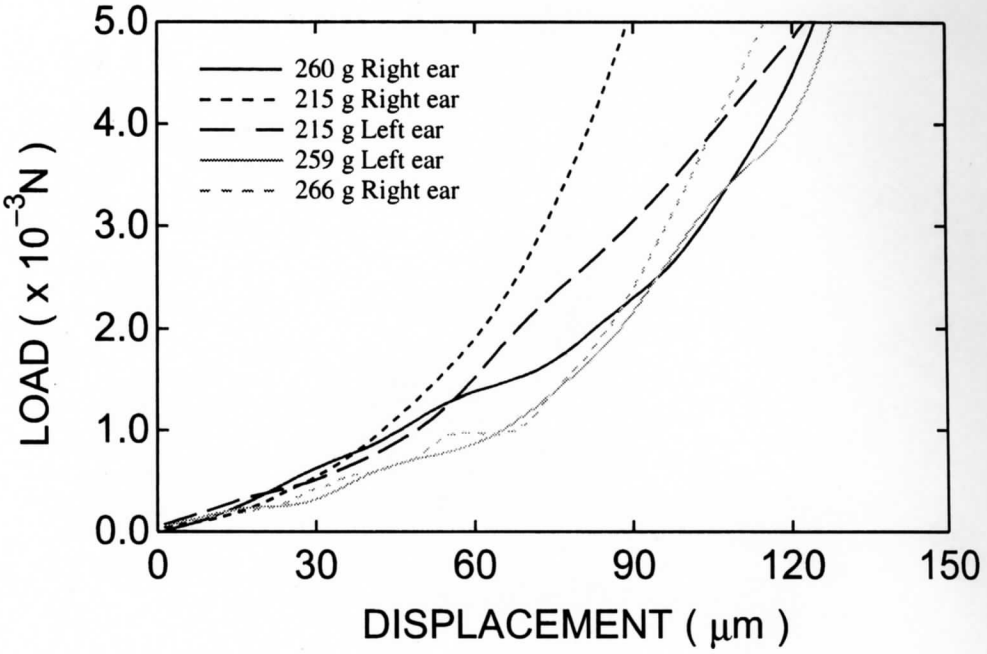

(b)

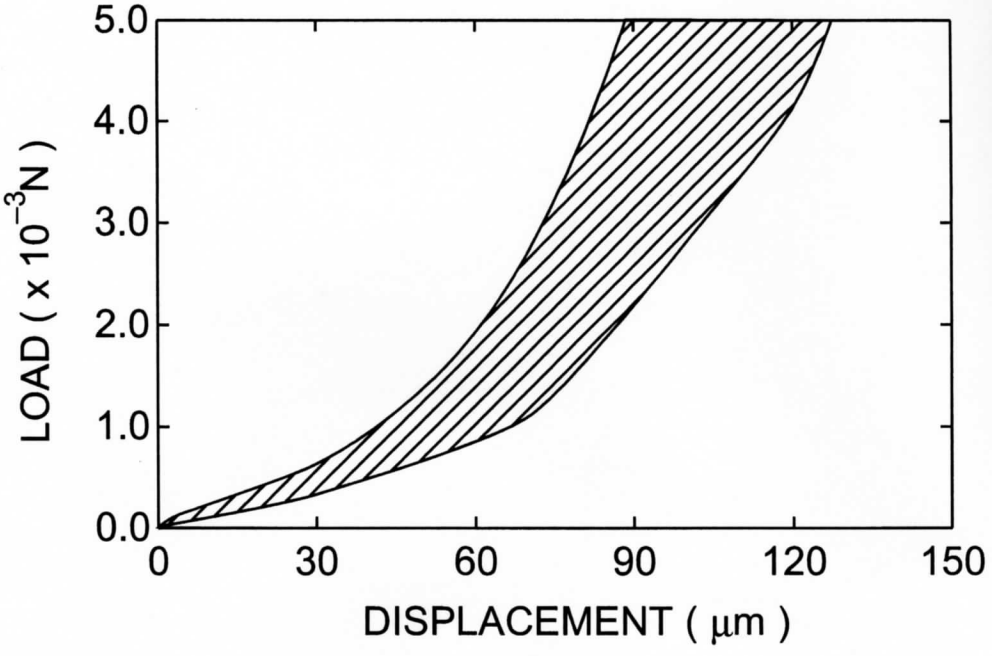

Fig. 5.3. Relationship between the load and displacement of normal stapes in guinea pigs measured by the new apparatus. Five temporal bones of four guinea pigs were used for the measurements. The measurements were done semi-statically. The pushing velocity of the actuator installed in the new apparatus was 650 μm/sec, the moving displacement of the actuator was 150 μm and the sampling frequency of A/D board was 500 Hz. The measurements took 0.23 sec. (a) Respective results. (b) The area in which all the measurement results were found. The average equivalent stiffness of all results was 17 ± 3 N/m (N = 5).

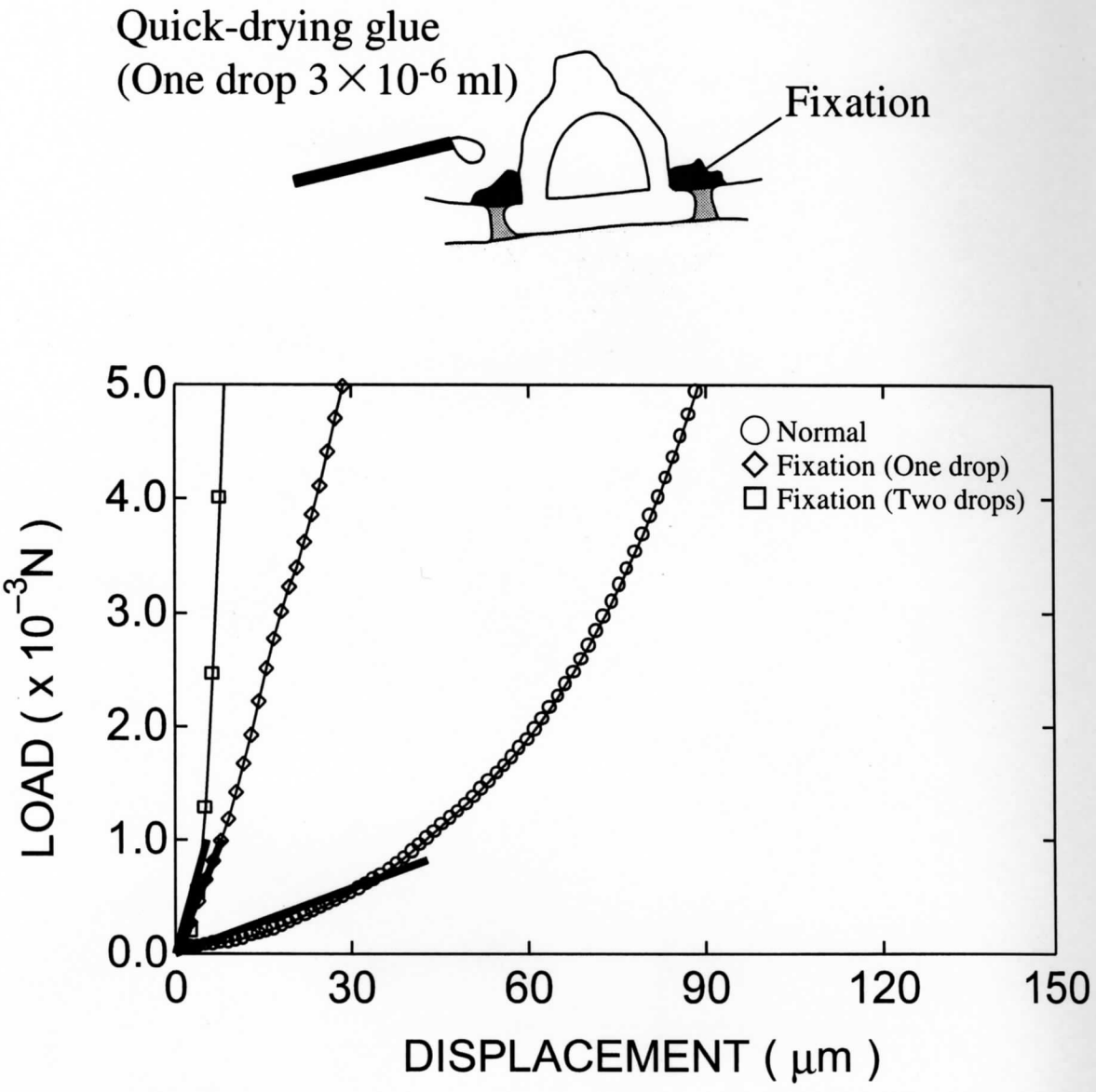

Fig. 5.4. Relationship between the load and displacement of the normal and artificially fixed stapes in a guinea pig measured by the new apparatus. The upper illustration shows the method of realizing stapes fixation. A temporal bone of a guinea pig was used for the measurements. The measurements were done semi-statically. The pushing velocity of the actuator installed in the new apparatus was 650 μm/sec, the moving displacement of the actuator was 150 μm and the sampling frequency of A/D board was 500 Hz. The measurements took 0.23 sec. The equivalent stiffness was 19 N/m in the normal stapes, 124 N/m in fixation created by one drop of the glue (3×10^{-6} ml) and 185 N/m in fixation created by two drops of the glue (6×10^{-6} ml).

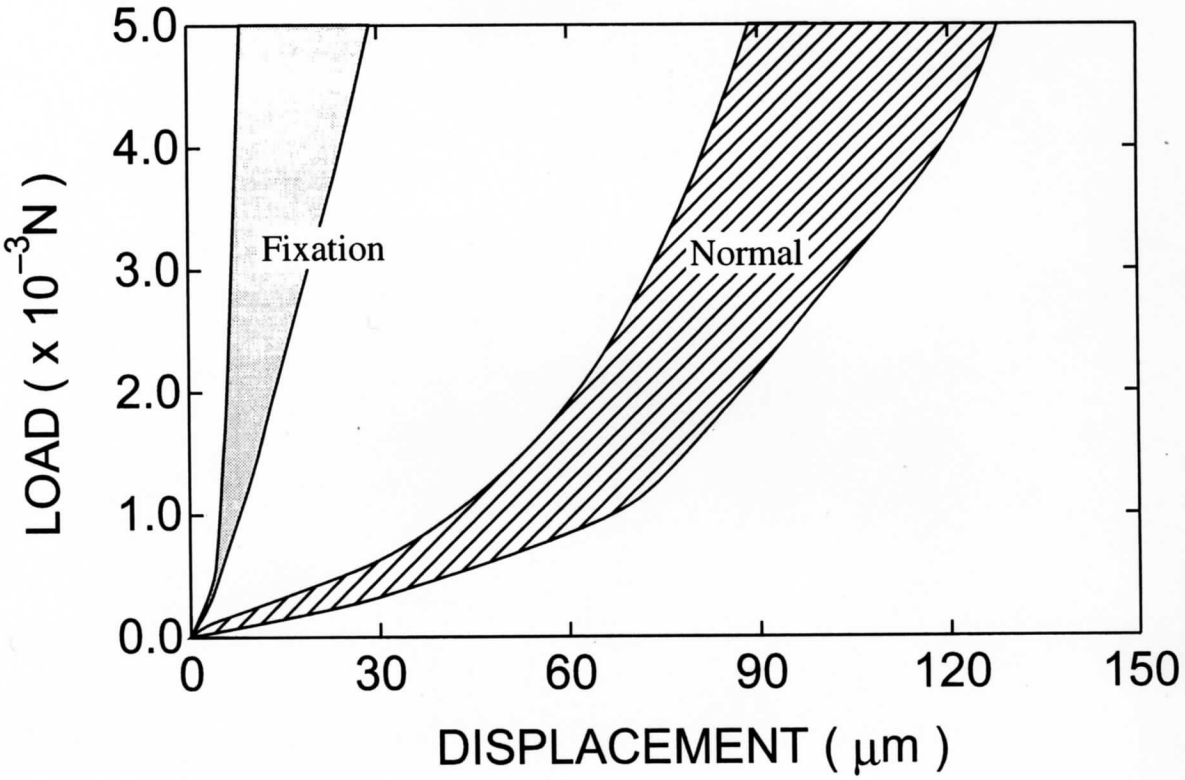

Fig. 5.5. Relationship between the load and displacement of normal and artificially fixed stapes in guinea pigs measured by the new apparatus. Five temporal bones of four guinea pigs were used for the measurements. The measurements were done semi-statically. The pushing velocity of the actuator installed in the new apparatus was 650 μm/sec, the moving displacement of the actuator was 150 μm and the sampling frequency of A/D board was 500 Hz. The measurements took 0.23 sec. All the measurement results of the normal stapes were found within the hatched area, and those of artificially fixed stapes were found within the gray area. The average equivalent stiffness of all results of normal and artificially fixed stapes were 17 ± 3 N/m (N = 5) and 151 ± 32 N/m (N = 5), respectively.

Chapter 6. Discussion

In this study on measurement of atapes mobility during surgery, we concentrated on miniaturizing the measurement apparatus. The new apparatus (Fig. 3.14) has a long thin probe and a grip. This shape enables measurement of stapes mobility through the external ear canal with the apparatus being held by hand, although such measurement is difficult in the case of the simple sensor which was used in the pilot experiments (Fig. 3.2).

A small-sized sensor and a driving system for moving the sensor, which consists of a hydraulic micromanipulator, a flexible coil, a rod and wires were developed to realize such a thin probe (Fig. 3.14). This mechanism is advantagiouse in the measurement of stiffness of other objects, because it is possible to change the sensor in conformity with measuring subjects.

The repeatability of stiffness measurement is shown in Fig. 5.2. The standard deviation of the equivalent stiffness was about 4% of its average. This value is thought to be sufficiently small compared with the individual difference. Therefore, the repeatability of the new measurement system is good enough.

Comparing Figs. 3.7 and 5.1, the relationship between the load and displacement of normal stapes in a guinea pig measured by the new apparatus corresponds to that measured by the simple sensor in the pilot experiment. Moreover, the area in which all the measurement results using the new apparatus were found and that obtained using the simple sensor well agreed for the small displacement region below 60 μm (Fig. 6.1). This means that the optimization of the shape of the apparatus for surgery was successful without impairing its function as a measuring device. In the

large displacement region above 60 μm, the load measured by the new apparatus tends to be larger than that measured by the simple sensor at a certain displacement. When the stapes mobilities were measured with the new apparatus, the temporal bone was used to simplify the measurements. By contrast, in the pilot experiment with the simple sensor, living guinea pigs were used. This may be one reason for that difference.

A significant difference was found between the equivalent stiffness before and that after the artificial fixation of the stapes in guinea pigs (Fig. 5.5). Moreover, a degree of stapes fixation in the guinea pig was detected (Fig. 5.4). These fixations, which were realized by deposition of a small amount of the alkyl-α-cyanoaerilate glue, correspond to the actual state of the stapes in the case of otosclerosis (Avan et al., 1992; Wada et al., 2000). Therefore, its clinical applicability for diagnosing stapes fixation in humans was suggested.

There have been few reports on the development of devices to measure stapes mobility in a clinical setting. Lau et al. (1963) developed an ossicular mobility checker for human, but the device did not become popular because the clinical significance of the device was not fully recognized. Recently, Gyo et al. (2000) developed a piezoelectric device for assessment of stapes mobility during surgery. The device comprised a pair of ceramic bimorph elements, and measured input impedance of stapes and cochlea. The evaluation of the device was done by measuring the input impedance of the normal and artificially fixed stapes in 5 ears of 5 dogs. They found a significant difference between the input impedance of the normal and artificially stapes. Hofmann et al. (1999) developed a hand-guided electromagnetic device. The input impedance of stapes and cochlea of human was measured by this device. And the

sensor's clinical benefit was confirmed by the 10 intraoperative measurements during ear surgery in patients with normal and fixed stapes.

The above techniques measure dynamic impedance of the stapes. The dynamic impedance consists of mass, stiffness and damping components (Onchi, 1961), and the stiffness component is dominant below 1 kHz (Merchant et al., 1996). Therefore, the results obtained from these techniques contain the effect of mass and damping, and to separate measurement of stapes stiffness is thought to be difficult. Consequently, the new apparatus developed in this study has the advantage of being able to effectively diagnose stapes fixation, because it can measure stapes mobility in a semi-static state.

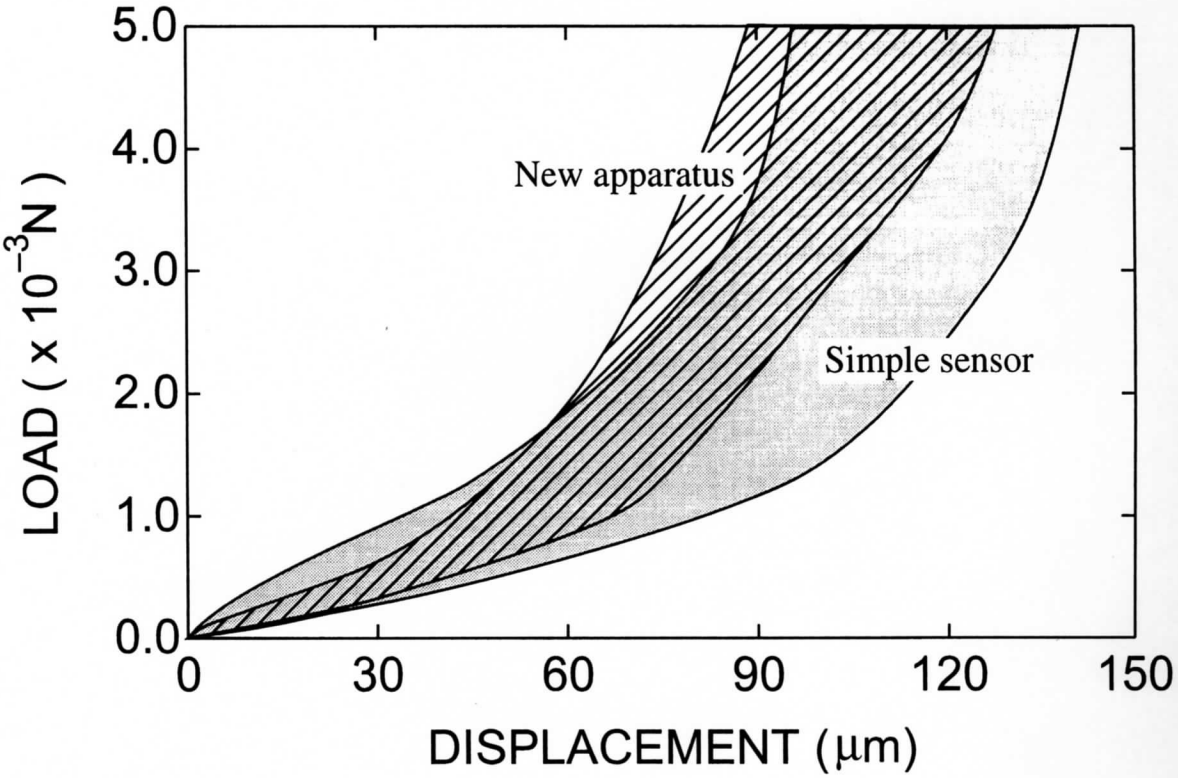

Fig. 6.1. Relationship between the load and displacement of the normal stapes in guinea pigs measured by a simple sensor (Fig. 3.1) and the new apparatus (Fig. 3.15). All the measurement results of normal stapes measured by the simple sensor are found within the gray area, and those measured by new apparatus are within the hatched area. The average equivalent stiffness of all results of normal stapes measured by the simple sensor and that measured by the new apparatus were 16± 7 N/m (N = 30) and 17±3 N/m (N = 5), respectively.

Chapter 7. Conclusion

With an eye on future clinical practice, an apparatus was developed and applied to the measurement of stapes mobility in guinea pigs. The following conclusions can be drawn.

1. Miniaturization of the apparatus was realized by the use of a small-sized capacitive force sensor and a hydraulic micromanipulator with a flexible coil rod and wires. Owing to this technology, the stapes mobility is measurable during surgery without impairing the sensitivity and repeatability.

2. The equivalent stiffness of the normal stapes in guinea pigs was 17 ± 3 N/m ($N = 5$). This result is in good agreement with that of a previous report (Wada et al., 2000).

3. The difference between the stiffness of the normal stapes and that of the artificially fixed stapes which corresponds to the symptom of otosclerosis was clearly distinguished. Therefore, the new apparatus developed in this study would be helpful for diagnosing stapes fixation.

Reference

Avan, P., Loth, D., Menguy, C. and Teyssou, M. 1992. Hypothetical roles of middle ear muscles in the guinea-pig. Hear. Res. 59, 59-69.

Bel, J., Causse, J. and Michaux, P., 1975. Paradoxical compliance in otosclerosis. Audiol. 14, 118-129.

Browning, G. G., Swan, I. R. C. and Gatehouse, S., 1985. The doubtful value of tympanometry in the diagnosis of otosclerosis. J. Laryngol. Otol. 99, 545-547.

Decraemer, W. F., Khanna, S. M. and Funell, W. R. J., 2000. Measurement and modelling of the three-dimensional vibration of the stapes in cat. In: H. Wada, T. Takasaka, K. Ikeda, K. Ohyama and T. Koike (Eds.), Proceedings of the international symposium on recent developments in auditory mechanics. World Scientific, Hong Kong, pp. 36-43.

江刺正喜, 藤田博之, 五十嵐伊勢美, 杉山進, 1992. マイクロマシーニングとマイクロメカトロニクス. 培風館, 東京.

Fujii, H., 2000. Development of measurement method of stapes mobility. Tohoku Univ. PhM thesis.

Gersdorff, M. and Stoquart, T., 1985. Phasor Diagram: A comparative study between normal ears and otosclerotic ears. Audiol. 24, 167-173.

Giovanni, M., 1982. Flat and corrugated diaphragm design handbook. Marcel Dekker, inc., New York.

Goodhill, V., 1979. Ear disease, deafness, and dizziness. Harper and Row, Hangerstown.